

# Assessment of an experimental ex vivo perfusion setup of ovine hearts based on pressure-volume analysis by a MATLAB model

*A collaboration between the University of Groningen, the UMCG and XVIVO*

Bart Wijntjes  
s3453030

Supervisor: dr. M.E. Erasmus  
Department of Cardiothoracic Surgery, UMCG

Daily Supervisor: F. Nijhuis  
Product Engineer, XVIVO

Examiner: dr. ir. R. Fluit  
Department of Biomedical Engineering, University of Groningen

Period: 17/04/2023 - 01/07/2023

# Contents

<b>1</b>	<b>Abstract</b>	<b>3</b>
<b>2</b>	<b>Introduction</b>	<b>4</b>
2.1	Literature review . . . . .	4
2.1.1	Heart failure . . . . .	4
2.1.2	Donor heart shortage . . . . .	4
2.1.3	Langendorff perfusion . . . . .	4
2.2	New experimental approach . . . . .	4
2.2.1	Pressure-volume curve . . . . .	5
2.2.2	PV related variables . . . . .	5
2.2.3	Measuring pressure and volume . . . . .	8
2.3	The experimental device . . . . .	8
2.3.1	Reference parameters . . . . .	9
2.4	Project aim . . . . .	10
<b>3</b>	<b>Methods</b>	<b>11</b>
3.1	Experimental prerequisites . . . . .	11
3.2	Data collection . . . . .	12
3.3	Data analysis . . . . .	12
<b>4</b>	<b>Results</b>	<b>14</b>
4.1	Calculated values of the model . . . . .	14
4.1.1	Secondary outcome parameters . . . . .	14
4.2	Graphical representation of the model . . . . .	15
<b>5</b>	<b>Discussion</b>	<b>17</b>
5.1	General assessment of the model . . . . .	17
5.2	Calculations of the model . . . . .	17
5.2.1	Calculation of $ESPVR$ . . . . .	17
5.2.2	Calculation of $E_{es}$ . . . . .	17
5.2.3	Calculation of $E_a$ . . . . .	19
5.2.4	Ratio $E_a/E_{es}$ . . . . .	20
5.2.5	Calculation of other parameters . . . . .	21
5.3	Limitations . . . . .	21
<b>6</b>	<b>Conclusion</b>	<b>23</b>
<b>7</b>	<b>Appendix</b>	<b>24</b>
7.1	Script of the developed MATLAB model . . . . .	24

# 1 Abstract

Transplanting a healthy heart into a patient is common treatment for chronic heart failure. However, donor hearts are not commonly available. Often donation after brainstem death (DBD) hearts are used and donation after circulatory death (DCD) hearts are put aside. However, DCD hearts could lead to a large increase of the donor pool, if properly assessed. Such assessment of the heart can be done based on pressure-volume (PV) measurement analysis. Especially contractility of the heart is a useful parameter in assessing the cardiac function before transplanting. The aim of this project was to develop a predictive model of contractility parameters of the heart based on PV-measurements of sheep hearts in a custom ex-vivo experimental setup. The model was developed in MATLAB and the main focus of the model was on calculating and visually representing the parameters end-systolic pressure volume ratio ( $ESPVR$ ), end-systolic elastance ( $E_{es}$ ), arterial elastance ( $E_a$ ) and the ratio  $E_a/E_{es}$ . These parameters were compared to reference values found in an extensive literature search. Parameters  $ESPVR$  and  $E_{es}$  were considered within an acceptable range of the reference values. Parameter  $E_a$  was calculated in two ways, the first by taking the mean of each cycle ( $E_a$ ) and the second by fitting a line between the  $EDV$  points and pressure maxima ( $E_{a_{fit}}$ ).  $E_{a_{fit}}$  was considered more accurate than  $E_a$  with respect to the reference values. The ratio of  $E_a/E_{es}$  for both types of  $E_a$  varied a lot, leading to the conclusion that further validation of the calculation of  $E_a$  is required before the model can be deemed accurate.

## 2 Introduction

### 2.1 Literature review

#### 2.1.1 Heart failure

Heart failure is becoming an increasingly large problem for Western healthcare [1]. Especially patients with complex diseases such as chronic heart failure are difficult to treat. Chronic heart failure is a multifaceted clinical syndrome resulting from abnormalities in the structure or function of the heart, which can be caused by ventricular systolic or diastolic disorders [1]. During systolic heart failure, the heart struggles to contract sufficiently for proper ejection. During diastolic heart failure, the heart struggles to relax enough for proper filling of the ventricle [2]. Patients with such advanced heart failure are often eligible for receiving a donor heart through transplantation as a final resort to treat them [3].

#### 2.1.2 Donor heart shortage

Although transplanting a new heart works as a good treatment for the heart failure patient, donor hearts are not commonly available. This is because donor hearts are mostly selectively available during donation after brainstem death (DBD). Even before being retrieved, these hearts already suffer from injury due to the inactivity of the brain, but the extent of the damage to the myocardium is sometimes uncertain [4]. Recently, so-called donation after circulatory death (DCD) hearts, can be transplanted as well. These DCD hearts come from donors where the heart's arrest is caused by anoxia after life support is withdrawn. For DCD hearts, ex situ function measurement, where the heart is out of its original place, is key as you often don't know the effect of anoxia and ischemia on these hearts. It has been estimated that including more DCD hearts can lead up to 30% increase of the donor pool worldwide [5]. Therefore the soon-to-be donor hearts should be properly assessed before being transplanted since a proper functional assessment method could increase the donor heart population [6].

#### 2.1.3 Langendorff perfusion

Preclinically, such assessment can be done by using Langendorff perfusion, in which the heart's muscles are perfused by blood in the coronary veins, without the ventricles filling with blood [7]. This ex situ method allows for either constant pressure or constant flow during perfusion. Coronary flow can be measured by collecting the flowing blood in a reservoir. Pressure can be measured by putting a pressure transducer in the blood circuit before the cannula enters the heart. The contractile function can be measured by measuring the linear contraction through the axis of the heart along a string that goes through the heart and comes out through the apex and leads to an isometric force transducer [7]. The string is encapsulated by a balloon that is placed in the left ventricle. Although useful, this method does not provide a complete picture of the contractile health of the heart, which leads to hearts being unnecessarily rejected. A method that could paint a more complete picture of the heart is therefore desirable.

### 2.2 New experimental approach

By looking at the volume exerted in the left ventricle (LV) of the heart as well as pressure, which is considered by some to be the benchmark approach for quantifying inherent chamber systolic and diastolic characteristics, one could obtain more information about the health of the heart [8]. This information could help save more hearts that are currently being rejected for transplantation based on the limited (pressure-based) analysis of the Langendorff method. Using the volume of the balloon during perfusion could be a clever way of getting a clearer representation of the heart's functionality. Plotting pressure and volume against one another leads to a so-called pressure-volume (PV) curve [9]. This curve describes the cardiac function of the LV and can thus be used as an indicator of how functional the heart still is.

### 2.2.1 Pressure-volume curve

An example of a PV-curve measured in vivo is given in Figure 1. In the right side of Figure 1, one can see the PV-curve of the LV, which follows a loop pattern. Generally speaking, the loop pattern has 4 phases: Ventricular filling, isovolumic/isovolumetric contraction, ejection and isovolumic/isovolumetric relaxation [8]. The mitral valve closure point, located at the bottom right corner of the loop in Figure 1, corresponds to the end of diastole when the pressure in the LV surpasses that of the atrium. This point is commonly known as the end-diastolic point. From that point, the isovolumetric contraction starts, whereby the pressure inside the LV rises at a constant volume until it surpasses the pressure of the aorta, leading to the opening of the aortic valve. This marks the onset of ejection. After reaching the peak systolic pressure, a gradual reduction in both pressure and volume initiates the slow ejection phase. This phase continues until the LV pressure falls below the aortic pressure, resulting in the closure of the aortic valve. This point in the cycle is referred to as the end-systolic point after which the diastole begins. During diastole, the myocardium ceases to contract and relaxes. As a consequence, there is a decrease in ventricular pressure at a constant volume, known as isovolumetric relaxation, which is followed by chamber filling that happens as the pressure increases [10].

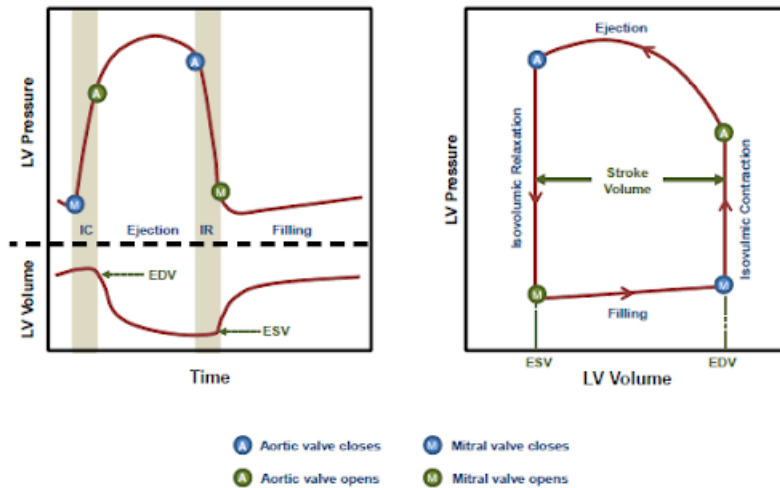


Figure 1: A standard example of an LV PV-curve [10].

### 2.2.2 PV related variables

From the PV-curve, one can derive functionality parameters of the heart. There are 3 principal factors or central characteristics of a PV-curve that govern LV performance and that can be divided into parameters: **Preload** can be characterized as the amount of blood in the LV at the end of the diastole and represents the load on the muscle fibres just before contraction [10].

**Afterload** or arterial impedance refers to external factors that resist the shortening of muscle fibres. Afterload can be represented by the variable  $E_a$ , the arterial elastance. This arterial elastance can be interpreted in a broad sense, representing all the complex mechanisms that result in a resistance against which the heart has to pump in order to achieve ejection.

**Contractile/ inotropic state of the myocardium** refers to the contractile force generated by the cardiac muscle fibres during each heartbeat. It is an important factor related to the functioning of the heart because it affects the parameter stroke volume ( $SV$ ).  $SV$  can be characterized as a parameter governing the functionality of the heart and represents the amount of volume the heart pumps during systole.  $SV$  can be derived by measuring the width of the PV-curve from end-diastolic volume ( $EDV$ ) to end-systolic volume ( $ESV$ ).  $SV$  becomes larger at higher preload due to the Frank-Starling effect. The Frank-Starling effect entails that if the heart is filled up more (for example at a higher preload) the heart walls stretch. This leads to an optimal muscle fibre length which increases the force of the contraction and therefore a larger

$SV$  coming out of the heart [11].

A second important parameter to assess contractile state is the ejection fraction ( $EF$ ), which can be calculated by  $SV/EDV$  and which represents the ratio of how much blood is pumped per stroke over the total amount of blood at the end of the diastole [10].  $EF$  is also affected by the Frank-Starling effect at variable load.

A third parameter is cardiac output ( $CO$ ) which quantifies the amount of blood pumped by the LV per time unit, i.e.  $SV/HR$  with  $HR$  being the heart rate [10]. Although useful, all the contractile parameters mentioned above are dependent on load of the LV, and thus are prone to perturbations as a consequence of load variability and the hearts Frank-Starling effect. Ideally, one would use load-independent parameters to characterize contractility to get the most accurate description of the cardiac function of the heart [10].

Cardiac function can also be assessed based on pressure measurements in the ventricles [7]. In this case, the parameters referred to are often  $dP/dt_{\max}$  and  $dP/dt_{\min}$  [10].  $dP/dt_{\max}$  is the maximum rate of pressure change and is known to be sensitive to the inotropic state which makes it related to the contractility of the heart.  $dP/dt_{\min}$  is the peak decline of pressure and can be used to give some quantification of the isovolumetric relaxation phase which is affected by high contractility. Unfortunately, given that pressure is very much affected by the pre- and afterload, for example, changes in afterload lead to alterations in either the timing of aortic valve closure or the peak aortic pressure, these parameters are not always good indices of contractility of the heart [10]. Another way of establishing something about isovolumetric relaxation is by looking at the decay in pressure from the moment of  $dP/dt_{\min}$  until the moment of end-diastolic pressure (EDP), which according to Weiss et al. can be characterized by the pressure formula  $P(t) = P_{dP/dt_{\min}} * e^{-t/\tau}$  [12]. In this formula time constant  $\tau$  is used which refers to the duration required for the pressure to decrease by approximately two-thirds of its initial value in the LV [10]. When isovolumetric relaxation becomes longer,  $\tau$  increases. Although  $\tau$  is independent of preload, it is still afterload-dependent in most animal model data, thus not a good indicator of contractility [13]. Nevertheless,  $\tau$  has been reported to be used for the quantification of relaxation.

Regardless of sensitivity to load, pressure indexes can still be linked to volume measurements to negate their load dependence. By adjusting preload conditions, it is possible to calculate how  $dP/dt_{\max}$  relates to the end-diastolic volume ( $EDV$ ). Controlling the preload of the PV can be done by Inferior Vena Cava (IVC) balloon occlusion [14]. Adjusting preload conditions yields a linear relationship  $dP/dt_{\max}$  vs  $EDV$  of which the slope provides a contractility index that is independent of preload and proportional to the ratio of  $E_{es}$  to  $T_{es}$  with  $E_{es}$  being the end-systolic elastance and  $T_{es}$  being the time to the end of the systole. Although  $T_{es}$  is load-independent and decreases when the contractility state goes up, it varies with  $HR$ , and thus has limited use as an index of the inotropic state [10]. This also affects the applicability of  $dP/dt_{\max}$  vs  $EDV$  given that this relation also depends on  $T_{es}$  and thus on  $HR$ .

$E_{es}$  is an interesting parameter for describing contractility given that it is independent of pre- and afterload and therefore a good indicator of systolic function and ventricular contractility [10]. It circumvents the issues of variability that load-dependent parameters have, making it useful for assessing the health of the heart objectively.  $E_{es}$  is closely related to the end-systolic pressure-volume relationship ( $ESPVR$ ) of which  $E_{es}$  is the slope. Bauer et al. found in their research with 18 sheep that  $E_{es}$  significantly decreased with acute ischemia, indicating  $E_{es}$  as a useful parameter to assess the health of the heart of possible ischemic damage [15]. As the contractility increases, the slope  $E_{es}$  remains the same, however, the line  $ESPVR$  moves up in the graph [10]. The  $ESPVR$  is constructed by using multiple PV loops with varying ventricular filling volumes and plotting a line connecting the end-systolic points of all PV loops as can be seen in Figure 2 adopted from Kameyama et al. where  $ESPVR$  is indicated as "End-systolic P-V line" [16].  $ESPVR$  can be related to heart failure, as was done by Ha et al., who found that heart failure reduces contractility and lowers the  $ESPVR$  line [14]. The origin of the  $ESPVR$  line can be indicated by  $V_0$  or the volume intercept, which describes the theoretic volume in the ventricle for which no pressure is developed [10].

In the same graph, one can also see the "End-systolic P-SV line" which stands for the end-systolic pressure stroke-volume relation [16]. The slope of this line is represented by the parameter  $E_a$  which represents the pressure of the arterial system against which the ventricle has to work in order to pump the blood into the

aorta.  $E_a$  increases with inotropic enhancement, as it depends on end-systolic pressure (ESP) [10]. It also depends on the amount of blood that the ventricle ejects into the arterial system. Moreover, when the aortic valve shuts, the pressure within the aorta is approximately equal to ESP while containing  $SV$ , thus  $E_a$  can then be described by  $E_a = ESP/SV$  [10]. The coupling between the ventricle and the arterial system is at equilibrium at the intersection point of the End-systolic P-V line ( $ESPVR$ ) and the End-systolic P-SV line. Typically, this point occurs at the end-systolic pressure point [10]. The graph also shows the "End-diastolic P-V curve" or end-diastolic pressure-volume relation ( $EDPVR$ ), which represents the plastic-elastic properties of the myocardium during the diastolic filling phase. As the ventricle fills up, the myofibrils stretch up, so in order to prevent deformation there is a development of increasing tension in the ventricle [10]. This tension represented by the  $EDPVR$  is also dependent on the wall thickness and  $V_0$  and grows exponentially at increasing pressure and volume.

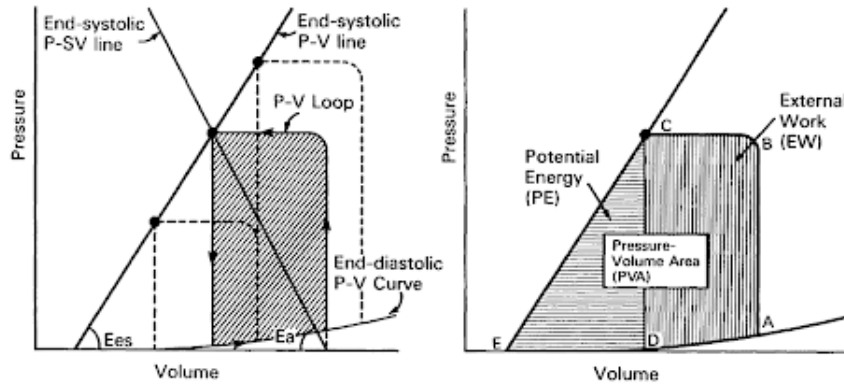


Figure 2: Graphs describing the  $ESPVR$ ,  $EDPVR$  and  $E_a$  (left) and the  $PE$ ,  $EW$  (or  $SW$ ) and  $PVA$  (right) [16].

In order to assess the functioning of the heart and the LV specifically, one can also focus on the efficiency of the LV in terms of energy. The parameter external work ( $EW$ ) or so-called stroke work ( $SW$ ) is the work done by the ventricle during contraction and describes work converted into hydraulic energy and stored in the ejected blood, which is then transferred to the arterial system.  $SW$  can be assessed by calculating the surface of the PV-loop. The transfer of energy is optimal when both chambers have the same elastance i.e. when  $E_a/E_{es} = 1$ . Although describing the mechanical efficiency of contraction of the LV with  $SW$  is intuitive, it is not the best indication of contractility given that  $SW$  is very sensitive to changes in preload [10]. Therefore, one can also compare the work of the LV with the total amount of energy of a ventricular beat, which is described by the Pressure-Volume Area ( $PVA$ ). The  $PVA$  characterizes the oxygen consumption of the LV and consists of the  $SW$  and the Potential Energy ( $PE$ ) of the LV [10].  $PE$  is the available mechanical energy in the LV at the end of the systole and is depicted as the triangle from  $V_0$  until point C which is the ESV intercept with  $E_{es}$  and point D which is the ESV intercept with  $ESPVR$  intercept in Figure 2. Once  $SW$ ,  $PE$  and  $PVA$  are calculated, one can infer things about the actual mechanical efficiency of the LV transferring the work of the LV to the arterial system, i.e.  $SW/PVA$ . This rate is known as the Cardiac Work Efficiency ( $CWE$ ) [10]. The heart must transfer an adequate amount of energy to the arterial system to fulfil its pumping function and maintain sufficient flow and perfusion pressure to operate as efficiently as possible. To accomplish this, the cardiovascular system aligns the ventricular and arterial properties to achieve optimal ventriculoarterial coupling for this function. Therefore,  $CWE$  is reciprocally related to  $E_a/E_{es}$ . Based on this, one can infer that  $CWE$  decreases with higher contractility and increases with higher afterload. Studies have shown that  $CWE$  is optimal when  $E_a/E_{es} = 0.5$  [17].

### 2.2.3 Measuring pressure and volume

#### 2.2.3.1 In situ functional measurement

Measurement of volume is often done *in vivo* where the heart is still in its original place or *in situ*. An advantage of this method is that the heart is still regulated by the body, making it possible to measure parameters of the heart under physiological circumstances. A disadvantage of this method is that accurate measurement of cardiac functionality often has to be done invasively, which can lead to complications [8]. A common *in situ* measurement method is using an invasive catheter that works with conductance. The catheter has multiple electrodes at a known distance and measures the high-frequency alternating current between the successive electrodes to obtain the cross-sectional area at the level of the electrode within the ventricle [8]. Summing the calculated areas up leads to the volume in the ventricle when it is in an isovolumetric phase. Pressure in this case is measured by a solid-state pressure sensor that is placed in the middle of the electrodes in the catheter [8, 15]. Although useful, this method relies on geometric assumptions about the size and shape of the heart and thus requires volume-related calibrations [18]. It is also limited by a potential nonlinearity in the relation between conductance and volume, especially when bigger volumes are involved [18].

An alternative method can be volume assessment by repeated or so-called *cine* Magnetic Resonance Imaging (MRI), which has been reported to yield more reliable estimates of LV volume [10]. An advantage of this method is that it can be done non-invasively. The downside of this method is that, while plotting PV-curves requires simultaneous measurement of volume and pressure, MRI interferes with the measurements of pressure. This is because the pressure signal can be distorted by the magnetic resonance. Furthermore, the pressure sensor can produce artefacts or noise on the MRI image [18].

#### 2.2.3.2 Ex situ functional measurement

*Ex situ* measurements are sometimes preferred for research purposes, given that they make the heart much more accessible for manipulations. Since the heart is out of the body, measurements performed on the heart are no longer invasive. However, since there is no brain and body to regulate the heart and blood anymore, *ex situ* setups are more prone to disturbances in oxygen and mineral regulation in the blood. Therefore, during *ex situ* measurements, the heart is often supplied with perfusate containing important substances such as glucose, insulin and epinephrine [19]. A significant downside of *ex situ* measurement, however, is that the myocardial function declines significantly during prolonged perfusion of the heart [19]. A common method for *ex situ* measurement is the Langendorff perfusion method [7]. Normally during Langendorff balloon measurement, only pressure measurements can be used to evaluate LV performance as was described in section 2.1.3. This is because the volume of the balloon is fixed, resulting in the isovolumetric measurement. In order to deal with the inaccuracies of measurement methods mentioned above, one could also use a less common method to measure the volume of the LV by use of a varying volume of the balloon. Such a method was developed by XVIVO.

## 2.3 The experimental device

The experimental device developed by XVIVO entails an inflatable conical balloon that is put into the LV of a heart via the left atrium *ex vivo*. The balloon is 90 mm in length and has a diameter of 70mm leading to a volume of approximately 100mL. The volume is constricted in growth by a 3D-printed black plastic cask which is attached to the mitral valve via a sutured knot. The plastic cask is put on a stainless steel cylinder with a piston which can be seen in Figure 3. The cylinder is then filled with a known amount of saline solution which is used to fill up the balloon, simulating an increase in preload. As the LV contracts, the volume is pushed out of the balloon into the cylinder, moving the piston. The back end of the device is connected to a wire motor which can be seen in Figure 3b. This wire motor responds to a TruWave pressure sensor catheter (TruWave Edwards Lifescience, Irvine, USA) that is placed at a known distance inside the balloon. As the piston moves, the tension in the wire changes which is picked up by the wire motor which moves to correct it, ensuring constant pressure. As the heart pumps, the piston moves according to the pressure in the LV. This movement of the position of the piston then moves through a Bowden-cable to the wire motor and can then be recorded by the wire motor which leads to volume data. The final PV- measurements are calculated with



regard to certain values which are preload, inverse compliance  $1/C$ , valve resistance  $R_v$ , distal resistance  $R_d$  and inertia  $L$  by an in-house software called 'Heart Assist-validator'. During isovolumetric phases, the motor speed is zero. During systolic ejection, the afterload is controlled by the software.

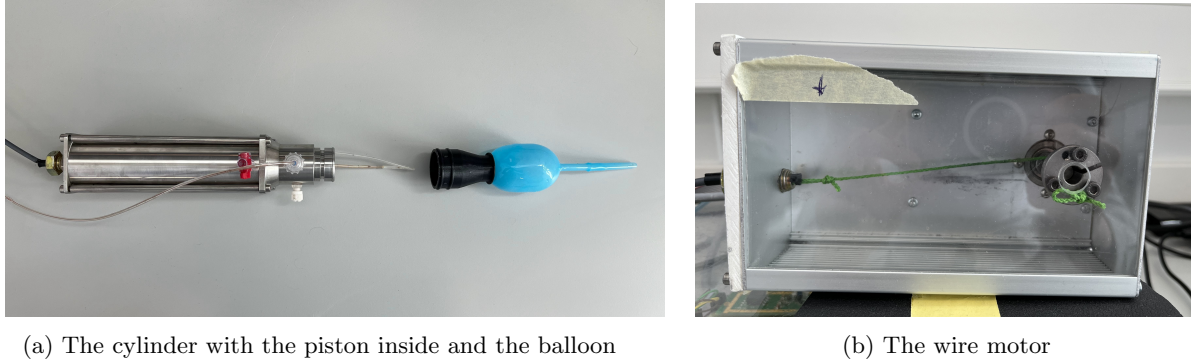


Figure 3: The cylinder-balloon setup and the wire-motor

Although promising, this experimental device still has to be validated in order to be considered a clinical method for assessing the health of the heart. In order to do so, it must be evaluated whether the pressure and volume data measured from the experimental setup are within the expected range of the pressure and volume of what would be expected based on literature.

### 2.3.1 Reference parameters

After stating all relevant parameters for PV-curve analysis, it is important to delineate the values of the reference parameters which will be used to compare the data of the experiments with. The hearts in the experiments are gathered from sheep, therefore ovine-based research is relevant. The found values from literature are depicted in Table 1. Segers et al. reported  $E_{es}$  of  $1.37 \text{ mmHg/mL}$ , a  $V_0$  of  $-36 \text{ mL}$ , and an EDV of  $79 \text{ mL}$  averaged over an  $n$  of 3 sheep at baseline [20]. When they used dobutamine ( $2 \mu\text{g/kg/min}$ ) for inotropic stimulation, they found an  $E_{es}$  of  $2.38\text{-}3.2 \text{ mmHg/mL}$ , a  $V_0$  of  $-21$  to  $-38 \text{ mL}$  and an EDV ranging between  $18$  to  $48 \text{ mL}$ . As can be seen from this research, dobutamine increases contractility parameter  $E_{es}$ , which has also been reported by research with other animals, such as dogs [21]. Romvari et al. mentioned an average EDV of  $43 \text{ mL}$ , ESV of  $11.2 \text{ mL}$ , SV of  $31.8 \text{ mL}$  and EF of  $77.9 \text{ mL}$  also based on 3 sheep [22]. Penny et al. also used dobutamine in their measurement to control the inotropic state in-vivo [23]. They measured a  $dP/dt_{\max}$  of  $1603 \text{ mmHg/s}$  at 0 dobutamine and  $3412 \text{ mmHg/s}$  at a dobutamine infusion rate of  $10 \mu\text{g/kg/min}$  [23]. Ha et al. compared multiple ovine heart experiments of several articles and found the following values as reference values: HR at  $88 \text{ min}^{-1}$ , SV at  $41 \text{ mL}$ , CO at  $3.6 \text{ min}^{-1}$ , ESP at  $105 \text{ mmHg}$ , EDP at  $3 \text{ mmHg}$ , a max LV elastance, which can be interpreted as  $E_{es}$  of  $1.37 \text{ mmHg} * \text{min}^{-1}$ , a  $dP/dt_{\max}$  of  $1345 \text{ mmHg} * \text{s}^{-1}$  and  $dP/dt_{\min}$  of  $-1226 \text{ mmHg} * \text{s}^{-1}$  [14]. Since they used the data of other articles, the  $n$  they used is not mentioned in Table 1. Bauer et al. measured 18 sheep for their cardiac parameters [15]. They reported an ESP of  $87 \text{ mmHg}$ , an  $dP/dt_{\max}$  of  $1346 \text{ mmHg/s}$  and an  $E_{es}$  of  $2.71 \text{ mmHg/mL}$  averaged over 4 healthy sheep. They also used 8 sheep who had had an old myocardial infarction (MI) 6 six months before measurement. For these sheep, they reported an ESP of  $94 \text{ mmHg}$ , an  $dP/dt_{\max}$  of  $842 \text{ mmHg/s}$  and an  $E_{es}$  of  $1.37 \text{ mmHg/mL}$  averaged over 8 sheep. Kelly et al. reported an  $E_a$  based on human PV measurement of  $0.35 \text{ mmHg/mL}$  at high preload and  $0.23 \text{ mmHg/mL}$  at lower preload [24]. Kameyama et al. also reported a mean human  $E_{es}$  of  $1.49 \text{ mmHg/mL}$  and  $E_a$  of  $2.55 \text{ mmHg/mL}$  [25]. Finally, Nishida et al. evaluated LV performance and measured parameters at a direct LV inflow with 7 healthy sheep [26]. They reported HR at  $104 \text{ min}^{-1}$ , SV at  $35 \text{ mL}$ , ESP at  $105 \text{ mmHg}$ , EDP at  $8.41 \text{ mmHg}$ , a  $E_{es}$  of  $1.2\text{-}1.8 \text{ mmHg/mL}$ , a  $E_a$  of  $1.3\text{-}2.3 \text{ mmHg/mL}$ , a  $dP/dt_{\max}$  of  $1012 \text{ mmHg} * \text{s}^{-1}$  and  $dP/dt_{\min}$  of  $-1040 \text{ mmHg} * \text{s}^{-1}$  [26]. Based on these measured parameters, the following estimated reference values can be set up as is shown in Table 2. Values with a '\*' are values that were calculated by averaging over the literature-based measurements mentioned above.

Table 1: Reference values from literature articles

	$E_{es}$	$E_a$	$EDV$	$ESV$	$EDP$	$ESP$	$V_0$	$dP/dt_{max}$	$n$
Segers et al.(baseline)	1.37	x	79	x	x	x	-36	x	3
Segers et al.(dobutamine)	2.38 — 3.2	x	18 — 48	x	x	x	17	x	3
Romvari et al.	x	x	43	11.2	x	x	x	x	3
Penny et al.	x	x	x	x	x	x	x	1603 — 3412	8
Ha et al.	1.37	x	x	x	3	105	x	1345	x
Bauer et al. (healthy)	2.71	x	x	x	x	87	x	1346	4
Bauer et al. (MI)	1.37	x	x	x	x	94	x	842	8
Kelly et al. (human)	x	-0.23 — -0.35	x	x	x	x	x	x	10
Kameyama et al. (human)	1.49	-2.55	x	x	x	x	x	x	13
Nishida et al .	1.2 — 1.8	-1.3 — -2.3	x	x	8.4	105		1012	7

Table 2: Reference values table

Parameter	Reference value range	Model reference value
$E_{es}$ ( $mmHg/mL$ )	1.2 — 3.2	1.4*
$E_a$ ( $mmHg/mL$ )	-1.3 — -2.3	- 2.3 [26]
$dP/dt_{max}$ ( $mmHg * s^{-1}$ )	842 — 1603	1229*
$dP/dt_{min}$ ( $mmHg * s^{-1}$ )	-1040 — -1226	-1133*
$ESP$ ( $mmHg$ )	87 — 105	95*
$EDP$ ( $mmHg$ )	3 — 8.41	8.4 [26]
$ESV$ ( $mL$ )	11.2	11.2 [20]
$EDV$ ( $mL$ )	43 — 79	70*

## 2.4 Project aim

The aim of this project is to develop a predictive model of contractility parameters of the heart based on pressure-volume (PV) measurements of sheep hearts in a custom ex-vivo experimental setup. In this model, the main focus will be on the end-systolic pressure-volume ratio ( $ESPVR$ ) and its slope which is the end-systolic elastance ( $E_{es}$ ). Both of these parameters are good indicators of ventricular contractility and systolic function because maximum elastance is independent of preload, afterload and heart rate [10]. Since contractility alone can not accurately assess the health of a heart ex-vivo, the parameter of arterial elastance ( $E_a$ ), which reflects the interaction between contractility and afterload [10], will also be calculated by the model. The ratio  $E_a/E_{es}$  can be used to quantify the coupling between the arterial system and the ventricle [10]. The total transfer of energy between chambers is optimal when  $E_a$  equals  $E_{es}$ . Therefore, the mechanical energy of the contraction of the ventricle, which is known as stroke work ( $SW$ ), is optimized when  $E_a/E_{es} = 1$ . By evaluating the mechanical efficiency of the work, one can infer things about the health of the heart and its contractility. However, since  $SW$  is very sensitive to preload, it is better to compare the energy transfer of the ventricle with regard to the total energy available, which can be represented by the pressure-volume area ( $PVA$ ). This comparison is described by the cardiac work efficiency ( $CWE$ ) [10] and reflects the proportion of the total generated energy that is actually converted to mechanical work for ejection of the stroke volume, thus describing contractility. Given the size of the reference  $E_a$  and  $E_{es}$ , an  $E_a/E_{es} = 1.64$  will be used as a reference value ( $2.3/1.5 = 1.6429$ ).

In summary, the model will entail calculations of the parameters describing contractility of the heart, focusing primarily on  $ESPVR$ ,  $E_{es}$ ,  $E_a$  and the ratio  $E_a/E_{es}$ . If time allows it, the model will also contain the parameters of  $SW$  and  $CWE$ . Furthermore, the model will compare the calculated values of the described parameters to literature-based values of healthy ovine hearts to validate the accuracy of the experimental setup.

## 3 Methods

### 3.1 Experimental prerequisites

The hearts used in the experimental setup are those of young sheep, no older than 2 years old. The hearts are immediately removed from the sheep carcass in the slaughterhouse along with at least 500 mL of blood to which heparin is added (5.000 IU/L). The heart has a short period of cardioplegia before being put on sub-normothermic perfusion (SMP). The blood used in the experimental setup is filtered through a cellsaver to remove coagulation factors and white blood cells and to increase the hematocrit. The blood is used during the experiment to perfuse the coronary arteries of the myocardium leading to the heart pumping. Venous blood coming from the coronaries is fed into the reservoir since the pulmonary artery is removed. During the experiments, the heart receives 4  $\mu\text{g}/\text{min}$  of dobutamine to improve inotropic state for better measurement. Dobutamine has an inotropic effect that increases contractility and overall cardiovascular performance, making differences in measurements of contractility clearer. The heart also receives an insuline/5% dextran mixture at a rate of 4.5 mL per hour. Every 15 minutes, a blood sample is taken to check the electrolyte levels and lactate in the blood. If needed, minerals such as  $\text{Ca}^{+2}$ ,  $\text{NaHCO}_3$  are administered to the reservoir to ensure the blood has the right properties, such as acidity, for the heart to function optimally. The experimental setup can be seen in Figure 4. During normothermic perfusion (NMP), the heart is placed on the sterile drape and attached to the oxygenated bloodline via a cannula in the aorta (here a. brachiocephalica) as is common in Langendorff perfusion [7]. The cannula is also used upon retrieval of the heart to flush it with HTK-solution [7]. The left a. carotis communis is used for the vent. The blood goes through the coronary veins to the right atrium, where it is pumped out onto the drape into the reservoir. From the reservoir, the blood is pumped via a centrifugal pump through an oxygenator supplying the blood with  $\text{O}_2$  at a rate of 0.1 L/min. In the lines of both oxygenated and low-oxygen blood is a temperature sensor to keep the temperature at the desired value by use of the Thermo Unit. Flow is measured in the arterial part of the system and can be set to a desired value. The pump unit gives the flow in mL/min, the pressure in mmHg and the temperature in degrees Celsius on a display.

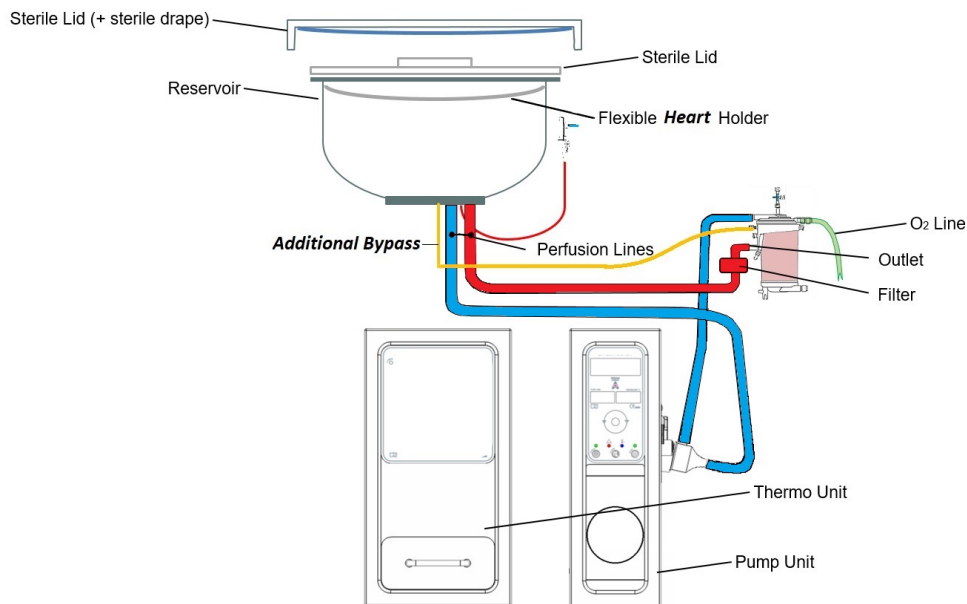


Figure 4: Experimental setup

Per heart experiment, two measurements are done at 1 hour and 2 hours after normothermic perfusion starts. Of these two, 1 will be included in the dataset, if the experiment progressed without any heavy perturbations or drastic cardiac irregularities. Before the start of normothermic perfusion, the heart is kept

subnormothermic at 15  $C^\circ$  during transport for up to 2 hours to reduce metabolism and limit ischemia of the heart when it is out of the body. During subnormothermic perfusion, the heart is flushed with PERFADEX<sup>®</sup> Plus and albumin. During normothermic perfusion, the temperature is gradually elevated to 37  $C^\circ$ , after which pacing is started to achieve a regular rhythm. The heart used should be large enough for the balloon to fit in the ventricle. If the ventricle of the heart is too small, the balloon will not properly inflate, leading to inaccuracy in volume and pressure measurements. Therefore, the hearts of younger sheep that could not contain the balloon were excluded from the data. The time between euthanasia and flushing of the heart was characterized as warm ischemic time. Warm ischemic time should be no longer than 9 minutes for inclusion of the heart in the experiment.

### 3.2 Data collection

The data from the experiments are gathered by use of the experimental setup shown in Figure 3. Measurements are collected and transported in log files in .csv format. Each log file contains the columns with the following headers: Timestamp, Volume ( $mL$ ), Pressure ( $mmHg$ ), Preload ( $mmHg$ ),  $1/C$ ,  $L$ ,  $R_v$ ,  $R_d$ , Fill Volume Phase, Aortic Pressure, End Systolic Pressure, Set Flow ( $mL/sec$ ), Flow ( $mL/sec$ ). Of these values, the values Preload ( $mmHg$ ), inverse compliance  $1/C$ , inertia  $L$ , valve resistance  $R_v$ , distal resistance  $R_d$  and Set Volume can be changed via a pop-up window on a laptop attached to the wire motor. These values are set up to reflect the afterload of the system and can be seen in Figure 5. In the figure,  $A$  is the aortic valve and  $GND$  are grounds. The afterload is governed by the following formula:

$$P = L \frac{dq}{dt} + q * R_p + \frac{1}{C} \int (q - q_{Rd}) dt + P_{C_0} \quad (1)$$

With  $L \frac{dq}{dt}$  as the mass inertia of the blood,  $P_{C_0}$  being the pressure at the start of the cycle,  $R_p$  the proximal resistance,  $q$  the flow into the aorta and  $q_{Rd}$  the distal flow out of the aorta. In this formula,  $\frac{1}{C} \int (q - q_{Rd}) dt$  represents the filling of the aorta during ejection.

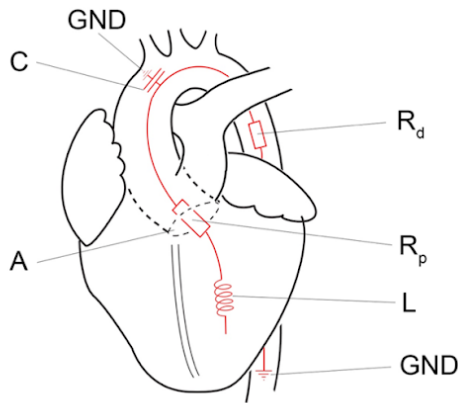


Figure 5: Schematic figure of how the afterload is modeled in the experimental setup.

All experiments are done under a  $1/C$  of 420, a  $R_v$  of 24.5, a  $R_d$  of 404.6 and a  $L$  of 0.7. These values are based on previous experiments [27]. One can alter the Set Volume based on how much volume is put into the cylinder during the experiment so that the volume measurement is accurate. As the experiment runs, the preload is changed every 10 seconds from 5 to 10 to 15 to 20  $mmHg$  in order to get multiple PV-loops of different sizes. These PV-loops can then be used for data analysis.

### 3.3 Data analysis

Analysis of the data will be done in MATLAB Version: 9.14.0 (R2023a) [28]. The MATLAB script will plot the pressure and volume data from the experiments and show the calculated  $ESPVR$ ,  $E_{es}$  and  $E_a$ . Further-

more, MATLAB will display the reference parameters based on literature in a separate graph.  $ESPVR$  will be obtained by using a similar method as Suga et al. [29]. The data presented there resembled square-shaped loops which allowed them to use the ESP-point of the consecutive PV-loops to obtain the  $EPSVR$  line. Since the ESP-points in their data also were the peak pressure points, the points used here to formulate  $ESPVR$  will also be the peak pressures of each cycle. This can be done by fitting a line through the maxima, using a first-order least-squares polynomial function (polyfit) [30]. The maxima in pressure were obtained after applying a low-frequency Butterworth filter to the data to eliminate noise. The filter used a sampling frequency of 60 and a cut-off frequency of 5. Then the cycles were extracted by use of a peak detection function 'findpeaks' in the pressure data [30]. Based on trial and error, a varying peak prominence between 30-50  $mmHg$  was used to obtain the pressure peaks from the data. This varying peak prominence was necessary due to differences in pressure to peak time in each cycle. At each peak, the data was run through a loop allowing for separate analysis. The polynomial was then fitted over all peak pressure to formulate  $ESPVR$ . The leading polynomial coefficient represents the slope of the fitted line, thus obtaining the  $E_{es}$ . The  $E_{es}$  of each experiment in the dataset will be compared to the reference values in order to evaluate the accuracy of the model.

$E_a$  will be obtained in a similar way as  $E_{es}$ . It will use the 'polyfit' function of MATLAB that has as input the EDV point before isovolumetric contraction and the ESP point [30]. Here, the ESP-points used are also the maximal pressures of a cycle, similar as in Monge Garcia et al. [31].  $EDV$  points will be obtained by taking the maximal volume within the cycle. It should be noted that this method could be sensitive to noise leading to an overestimation of  $EDV$ . The fitted line will be obtained by the MATLAB 'polyfit' function of which the first 2 coefficients will be used to obtain the slope  $E_a$  and its y-axis intercept [28]. Given that  $E_a$  is typically calculated based on single beat measurement, a separate parameter  $E_{a_{fit}}$  will be calculated to obtain the average  $E_a$  of the total measurement [32]. Continuing with  $E_a$ , the slope and y-axis intercept of each cycle will be stored in separate variables of which the means will be obtained using MATLAB's 'mean' function [30]. The mean slope  $E_a$  and y-axis intercept will then be used to plot the  $E_a$  line in the graphs.  $E_{a_{fit}}$  will be obtained by fitting a linear curve between the maximal pressure points of all cycles and the EDV points of all cycles. This will lead to a linear curve fitted over the entire measurement duration, leading to a different slope  $E_{a_{fit}}$ . Once  $E_a$  and  $E_{a_{fit}}$  are obtained, the ratio  $E_a/E_{es}$  can be obtained, which should approximate 1 to have optimal energy transfer between chambers [10]. The same comparison will be done for  $E_{a_{fit}}/E_{es}$ . If the ratio approximates 0,5, this would be indicative of an optimal  $CWE$ , meaning that although transfer over energy between chambers is not optimal, the coupling between the arterial system and the ventricle is still adequate for proper functioning.

Secondary parameters stroke volume ( $SV$ ) and stroke work ( $SW$ ) will also be calculated by the model to give an indication of how big the average exerted amount of volume and energy was during the experiments.  $SV$  will simply be calculated by taking the  $EDV - ESV$  of each cycle and taking the average of all cycles.  $SW$  will be calculated as an estimation of the surface of the PV-cycle by the formula  $SW = SV/(ESP - EDV)$ , which was averaged over all cycles.

Of all experiments, a total of 5 experiments were selected as input for the model. From these experiments, Excel data was generated by the computer in the experimental setup with a size of around 20.000 samples at a rate of approximately 4  $ms$  per sample. Experimental remarks regarding the conditions of the hearts can be found in table 5.

## 4 Results

Results were generated by the developed MATLAB model of which the script can be found in the Appendix section 7.1. A total of 5 ovine hearts were used as input for the model. The pressure and volume data were filtered before analysis. The hearts varied in size and weight, potentially leading to differences in calculated parameters. Further information about the heart retrieval from the sheep can be found in Appendix Table 5.

### 4.1 Calculated values of the model

The calculated values from the model can be seen in Table 3. Although  $EDV_{avg}$ ,  $ESV_{avg}$ ,  $EDP_{avg}$  and  $ESP_{avg}$  are secondary parameters to the model, they were represented here because of their relevance in the calculation of the  $ESPVR$  and  $E_a$  lines.

Table 3: Output of the model

Measurement	Date	$E_{es}$	$E_a$	$E_{a_{fit}}$	$E_a/E_{es}$	$E_{a_{fit}}/E_{es}$	$EDV_{avg}$	$ESV_{avg}$	$EDP_{avg}$	$ESP_{avg}$
1	14-03	0.946	-14.297	-8.227	15.112	8.696	20.112	8.713	21.711	108.014
2	18-04	3.398	-16.550	-4.156	4.870	1.223	12.867	4.587	15.898	80.609
3	25-04	2.683	-20.545	-11.282	7.657	4.205	57.486	48.069	14.963	104.212
4	09-05	-0.103	-16.343	-7.619	159.312	74.272	59.947	46.720	35.934	162.35
5	23-05	4.307	-19.341	-4.04	4.490	0.938	42.450	35.363	13.543	73.010
Reference	No date	1.4	-2.3	-2.3	1.64	1.64	70	11.2	8.4	95

As can be seen from Table 3, the hearts varied quite a lot in terms of calculated parameters. Measurement 1 showed the most resemblance with the reference  $E_{es}$  of 1.4 with a calculated  $E_{es}$  of 0.946. However, the  $E_a$  and  $E_{a_{fit}}$  of this measurement were much higher than the reference value of  $E_a$ , which was set to -2.3. Furthermore, the calculated  $E_{es}$  of measurement 4 was -0.103, which indicates a negative slope, making the model incapable of calculating an accurate  $V_0$ . Notice that the measured pressure here is also higher than during the other experiments, reaching almost 170  $mmHg$  while the others stay closer to 100  $mmHg$ . Measurements 2 and 5 were the closest in terms of  $E_{a_{fit}}$  to the reference value of  $E_a$ , with an  $E_{a_{fit}}$  of 4.156 and 4.04 respectively. Both of these measurements were also the closest to the reference  $E_{a_{fit}}/E_{es}$  of 1.64 with measurement 2 having a calculated value of 1.223 and measurement a value of 0.938. Regarding the proper calculation of  $E_a$ , the values calculated by the model of  $E_{a_{fit}}$  come closer to the reference value of -2.3 than the values of  $E_a$ , with a mean  $E_a$  of -17.415 and a mean  $E_{a_{fit}}$  of -7.2164.

$EDV_{avg}$  also differed among experiments, with experiment 3 being closest to the expected reference  $EDV$  of 70  $mL$  with an  $EDV_{avg}$  of 69.194. Measurements 1 and 2 were the furthest away from the reference  $EDV$  with an  $EDV$  of 20.112 and 12.867 respectively. These experiments performed better at approximating the reference  $ESV$  of 11.2  $mL$  at an  $ESV_{avg}$  of 8.713  $mL$  for measurement 1 and 4.587  $mL$  for measurement 2.  $EDP_{avg}$  was not calculated accurately relative to the reference model with measurement 5 coming closest to the reference  $EDP$  of 8.4  $mmHg$  with a calculated value of 13.543  $mmHg$ . Finally,  $ESP_{avg}$  was calculated to be closer to the reference  $ESP$  of 95  $mmHg$ , with only measurement 4 having a high calculated  $ESP_{avg}$  of 162.35  $mmHg$ .

#### 4.1.1 Secondary outcome parameters

Secondary outcome parameters that the model generated were  $SV$ ,  $SW$  and  $V_0$ . The calculated values of the parameters can be seen in Table 4. All three parameters were calculated for each cycle and then the average of all cycles was represented in the table.  $SV$  over all experiments had an average of 9.882  $mL$ .  $SW$  over all experiments had an average of 895,24  $J$ .  $V_0$  over all experiments had an average of -17.425  $mL$ , excluding

the  $V_0$  of measurement 4. Given that these were secondary parameters to the model, no further analysis of these parameters was done in this project.

Table 4: Secondary parameters  $SV, SW$  and  $V_0$

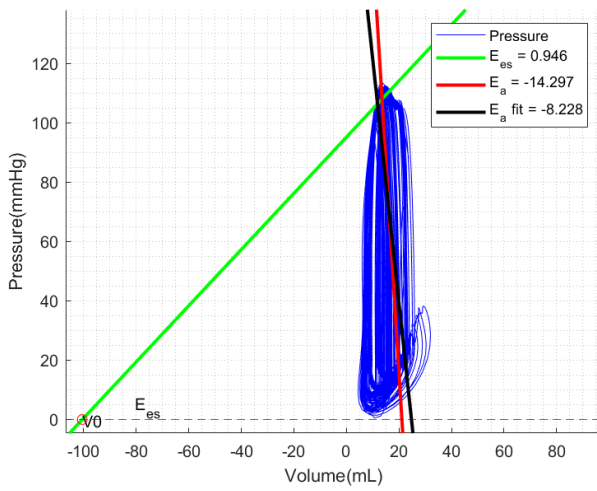
Measurement	Date of measurement	$SV$ (mL)	$SW$ (J)	$V_0$ (mL)
1	14-03	11.399	1000.6	-100.572
2	18-04	8.281	537.3	-14.845
3	25-04	9.417	840.707	14.263
4	09-05	13.228	1.673.000	x
5	23-05	7.086	424.610	31.452
Average	x	9.882	895.24	-17.425

## 4.2 Graphical representation of the model

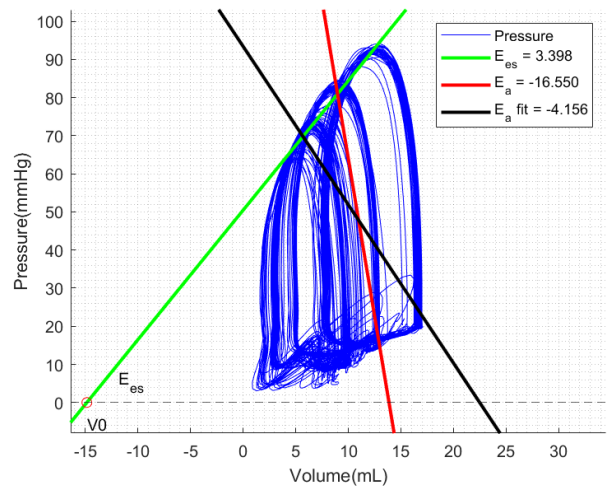
In Figure 6, one can see the figures generated by the model. The axis sizes vary for proper representation of the legend and the plotted pressure. The  $ESPVR$  is represented by the green line with  $E_{es}$  values indicated in the legend. The  $E_{a_{fit}}$  and  $E_a$  are indicated by the black and red lines, respectively.

First, looking at the  $ESPVR$  line which determines the  $E_{es}$ , one can see the slope differences between the measurements. Especially in Figure 6d, one can see that the  $ESPVR$  line does not have the proper slope for it to be able to cross the volume axis at a  $V_0$ . The slope should be positive, not negative in order to lead to a graph such as can be seen in Figure 2. The other measurements still cross the volume axis but at quite different volumes, therefore, the volume axes are different for each measurement in order to still be able to properly represent the cycles under different preload.

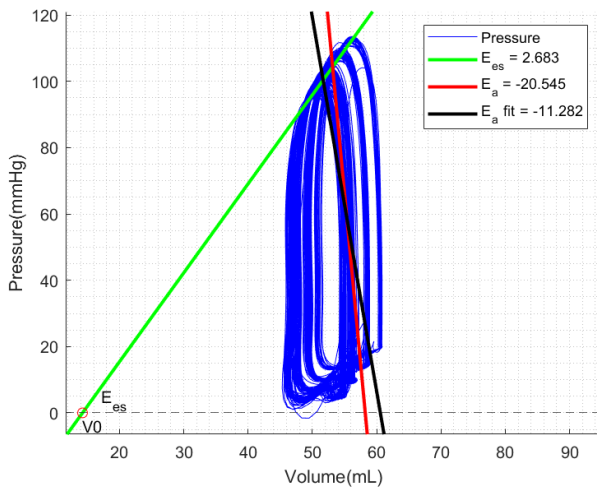
The  $E_a$  line, represented by the red line is generally steeper than the  $E_{a_{fit}}$  line and therefore has a more negative slope. Given that the reference slope was chosen to be around -2.3, this often leads to a higher deviation of the  $E_a$  from the reference value compared to  $E_{a_{fit}}$ . Especially when one compares them to the red line in the Reference measurement graph in Figure 6f, it seems that the  $E_{a_{fit}}$  lines come closer towards the slope one would expect  $E_a$  to have. However, looking at the Table 3, one can see that although both  $E_a$  and  $E_{a_{fit}}$  seem to have a slopes that are too negative, if one looks at the ratio of  $E_a/E_{es}$ , these differences are smaller than the graphs might suggest. Further interpretation of the results can be found in section 5.



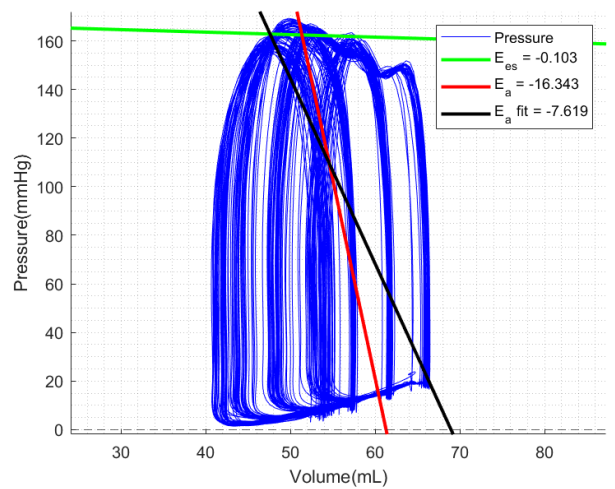
(a) Measurement 1



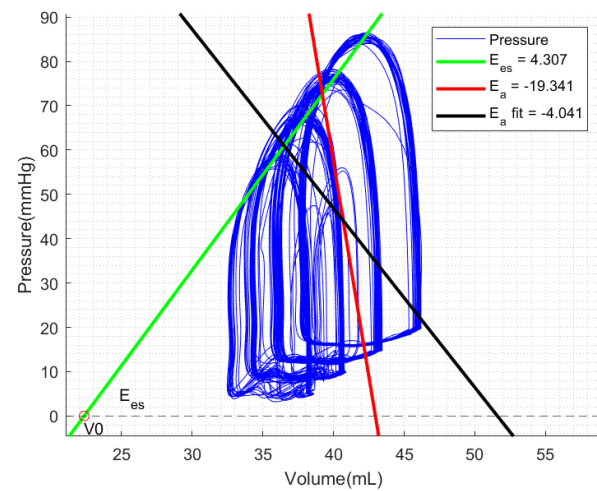
(b) Measurement 2



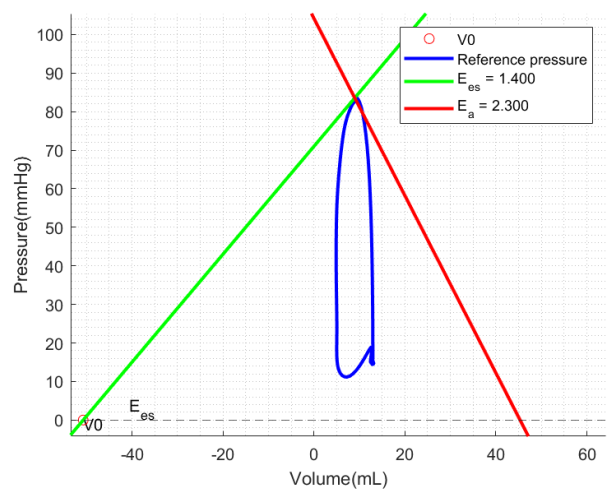
(c) Measurement 3



(d) Measurement 4



(e) Measurement 5



(f) Reference measurement

Figure 6: Generated figures of the ovine hearts after data analysis



## 5 Discussion

### 5.1 General assessment of the model

In general, the aim of the model was to provide predictive contractility parameters of the heart based on left ventricular pressure-volume measurements of sheep hearts derived in a custom ex-vivo experimental setup. The main focus of the model was to extract the  $ESPVR$ ,  $E_{es}$ ,  $E_a$  and the ratio  $E_a/E_{es}$  from the PV-data and represent them graphically. Secondary parameters that could be derived from the data were  $EDV$ ,  $ESV$ ,  $EDP$ ,  $ESP$ ,  $SV$ ,  $SW$ ,  $V_0$  and  $CWE$ . Except for  $CWE$ , all of the parameters were calculated and represented in the results. However, due to the 10-week time constraint of this project, the secondary parameters were not used for further interpretation in assessing the cardiac functionality of the measured hearts.

### 5.2 Calculations of the model

Although the calculations executed by the model were based on methods from other articles, there is still some room for improvement in terms of accuracy. In this section, the calculations of the various parameters will be discussed.

#### 5.2.1 Calculation of $ESPVR$

Concerning the  $ESPVR$ , it should be noted that the  $ESPVR$  in this model has been calculated by use of the maximum pressure point of each cycle and not the ESP-point of each cycle as has been done by others [10]. The maximum pressure points were chosen because the ESP-points were not clearly separable from the data gathered in the 5 experiments. Additionally, the experimental setup uses a piston that moves through stainless steel which has a certain impedance to simulate the preload in the heart. This is quite different to the aorta valve that is normally present in the heart, which can quickly open and close, leading to a steeper drop in pressure and a clearer separable ESP-point in the data. Because the experimental setup does not allow for such quick changes in pressure, using the maximal pressure points was considered an acceptable alternative.

The maximal pressure points were obtained by selection based on peak heights. Given that pressure peaks varied in terms of width, varying peak height or prominence was used. This was to make sure that the peaks that were picked up by the model were indeed peaks in the PV-curve instead of the smaller peaks caused by signal fluctuations that remained after filtering the data. However, in order to have a proper comparison between the hearts that are measured, you would preferably have measurements with equal peak height or with a peak selection based on a sample size that varies consistently. In general, the best peak selection of the data collected in the experiments was at a minimal peak prominence (or height difference) of 50  $mmHg$ .

#### 5.2.2 Calculation of $E_{es}$

The calculations of  $E_{es}$  were considered to be in an acceptable range, based on the limited range of values (-0.103 to 4.307) which is only slightly broader than the reference value range in Table 2. Measurement 1 had a calculated  $E_{es}$  of 0.946, which was the closest of all experiments to the reference value of 1.4. This is likely because the heart showed little difference in  $EDV-EPV$  at increasing preload. One explanation for this could be that this was caused by the prolonged perfusion time. Since this measurement was done after 2 hours, the heart could have become stiffer, leading to less volume filling the ventricle, thus less high pressures [19]. The result is that the peak points lie closer together, thus leading to a more constant slope approaching 1  $mmHg/mL$ . Note that an  $E_{es}$  of 1 does not mean that the heart has a good mechanical efficiency since this is only the case if the ratio  $E_a/E_{es}$  approaches 1. An  $E_{es}$  of 1 simply means that the  $ESPVR$  rises with 1  $mmHg$  per  $mL$ . For optimal transfer of energy between the chambers, the  $E_a$  of this measurement should also approximate 1.

Measurement 4 had a negative  $E_{es}$  of -0.103. This is odd given that  $E_{es}$  is expected to have a positive slope [10]. A possible explanation of this heart standing out in terms of  $E_{es}$  is perfusion fatigue. The heart

was relatively large and therefore the balloon was filled with a lot of volume. This might also explain why the pressure in this heart reached 160 *mmHg*, when it normally should not exceed 100-120 *mmHg* during regular functioning [33]. The combination of the large LV volume and long exercise for the heart during perfusion can eventually lead to heart failure, which was likely the case during the measurement of this heart [19, 34]. If this is the case, the model should indeed give an unexpected value for  $E_{es}$ , since the heart in this measurement was no longer a healthy heart, but a failing heart. Therefore, this finding could be interpreted as a demonstration that the calculated  $E_{es}$  is working as expected in describing the cardiac functionality of healthy hearts, while also being of use in identifying failing hearts.

The  $E_{es}$  was calculated by extracting the first coefficient from the linear curve function that was fitted by the 'polyfit' function of MATLAB [30]. This coefficient represented the slope of the fitted line. It should be noted that since the *ESPVR* was a fitted curve, this slope is only an approximated value and should be interpreted as such. Still, this method is similar to the ones used in other research. For example, a similar method of calculating  $E_{es}$  was used by Bauer et al., who measured the peak positive of the LV  $dP/dt$ . They determined the ESP at the upper points of the PV-curve for at least 12 curves and then applied a linear regression to obtain *ESPVR* [15]. This is effectively the same method for selecting ESP points as used here in the developed model.

End-systolic elastance  $E_{es}$  could also be used to calculate the general elastance of the heart. This general elastance can be obtained by using the method of Segers et al. They obtained the  $E_{es}$  by calculating the slope of the *ESPVR* [20]. They used this to set up a time-variant elastance model  $E(t)$ , representing the coupling between LV pressure ( $P_{LV}$ ) and LV volume ( $V_{LV}$ ) leading to the following formula:

$$E(t) = \frac{P_{LV}(t)}{V_{LV}(t) - V_d} \quad (2)$$

Here  $t$  represents time and  $V_d$  represents the intercept of the *ESPVR* with the volume axis, which is the same as  $V_0$ . This leads to a ratio which represents the contractility of the LV. They normalized this  $E(t)$  with respect to the maximal elastance  $E_{max}$  or  $E_{es}$  to get normalized elastance  $E_N(t) = E(t)/E_{max}$ . They then normalized time  $t$  towards the  $t_p$ , which is the time to reach peak elastance leading to  $t_N = t/t_p$  [20]. The result from this is  $E(t_N)$  which leads to curves that have been reported to have similar shapes for different inotropic conditions in both healthy subjects and subjects with cardiovascular deficiencies [29]. Thus, if one knows  $E(t_N)$ , one can easily determine the coupling between  $P_{LV}$  and  $V_{LV}$  using  $E_{max}$ ,  $t_p$  and  $V_d/V_0$ . This might be a more accurate use of the measured information within the data than the method used in the model developed in this project since the method of Segers et al. uses the  $V_0$  and time to reach peak elastance. Further research should investigate how well this general elastance represents cardiac function, also in comparison to the  $E_{es}$  used in this model.

Another interesting method was used by Takeuchi et al., who fitted a sinusoidal wave to the isovolumetric segments of the LV pressure waveforms for estimating maximal isovolumetric pressure, the  $P_{max}$  [35, 36]. They selected the ESP by locating the left upper corner of the PV-curve for 3 cycles per patient under different loading conditions to set up the *ESPVR* line and calculate the corresponding  $E_{es}$ .

Takeuchi et al. used  $dP/dt$  to estimate pressure curve segments from *EDP* to  $dP/dt_{max}$  and from  $dP/dt_{min}$  to the same level as *EDP* [35]. *EDP* itself was defined as the pressure at which  $dP/dt$  first crossed the threshold of 200 *mmHg/s* [35]. Then, the segments were used for the least-squares fitting of the sinusoidal function [36]. Kjørstad et al. took on a similar approach as Takeuchi et al. by using a fifth-order polynomial instead of a sinusoidal wave to account for the fact that there could be a discrepancy between the rate of pressure increase during isovolumetric contraction and the rate of pressure decrease during isovolumetric relaxation [37]. Nevertheless, they eventually found their methods failed to detect an increase in contractility in vivo and concluded that it needed more research [37]. Whether their methods would be viable for ex vivo measurement also remains to be determined.

The experimental setup measured different sized PV-loops with a changing preload at a constant dobutamine infusion of 4  $\mu\text{g}/\text{min}$ . However, it would also be interesting to see how the heart responds to titrating extra dobutamine as Sunagawa et al. did in their experiment [38]. They started at a dobutamine infusion of 10  $\mu\text{g}/\text{min}$  and increased infusion until they saw a 20% increase in  $E_{es}$ . This would be an interesting experiment

to determine if the  $E_{es}$  of the model responds to this in a similar fashion in order to validate its calculation. Additionally, it would also be interesting to check how large the influence of dobutamine is on the calculated  $E_{es}$  of the developed model.

### 5.2.3 Calculation of $E_a$

Arterial elastance  $E_a$  can be interpreted as arterial load, which describes the extracardiac factors that oppose the ejection of volume in the LV [39]. The most accurate description of arterial load is provided by aortic input impedance, which describes the relationship between pulsatile pressure and flow in the frequency domain and can be characterized by their respective amplitudes and phases [40]. Sunagawa et al. proposed that all components of arterial impedance could be integrated under the variable  $E_a$  [41]. This  $E_a$  does not represent a true physical elastance or arterial stiffness, but is an operative measure describing the primary features of the arterial system, such as impedance, compliance and resistance. In this model,  $E_a$  was interpreted as representing the complex load of the arterial system against which the heart has to pump in order for proper ejection of the LV to take place. This definition is rather broad and is different from Sunagawa's conception of  $E_a$ . The difference stems from the fact that the simplified definition of Sugawa does not account for the different contributions of pulsatile and steady flow and is therefore also not complete in describing  $E_a$ . The  $E_a$  from the model is therefore more broadly defined given that these parameters of steady and pulsatile flow are also not explicitly defined in the experimental setup, but are of influence on the final  $E_a$ . What can ultimately be read from this, is that there is still research to be done in finding the proper definition for arterial elastance  $E_a$ .

Concerning the  $E_a$  calculations in the developed model,  $E_a$  was calculated in two ways, since it is generally derived based on a single heartbeat or heart cycle and the data used here consisted of multiple cycles. The first method constituted parameter  $E_a$ , which was derived by calculating  $E_a$  for each beat or cycle. After calculation per beat, the mean was taken of the  $E_a$  of all cycles. This method is in line with the standard approach of calculating  $E_a$  based on a single-beat measurement since it calculates the  $E_a$  for each beat [10]. However, taking the mean as an eventual outcome might not be the best value to compare to the reference  $E_a$  given that the reference value was based on the  $E_a$  of a single beat from multiple different articles. Still,  $E_a$  can be useful to deduce the ratio  $E_a/E_{es}$  in order to infer things about the transfer of energy within the heart, which will be discussed in section 5.2.4.

$E_{a_{fit}}$  was found to be closer to the reference value of -2.3 than  $E_a$ , indicating that the calculation of  $E_{a_{fit}}$  was more accurate based on values found in literature [24, 25, 26]. However, the method of calculating  $E_{a_{fit}}$  using a large amount of cycles, is not the way  $E_a$  generally is calculated given that it in general only 1 to 12 beats are used [10, 31]. The model calculated  $E_{a_{fit}}$  by taking the peak pressure points of each cycle and the pressure points at  $EDV$  and fitting a linear function through the points with the same fitting function as used for  $E_{es}$ .

Furthermore, the  $E_a$  values here were calculated with the same pressure peaks as the  $E_{es}$ , which as mentioned, are not the same as ESP. Other research, such as that of Monge Garcia et al., uses surrogate pressures [31]. These pressures can include 90% of the systolic arterial pressure (SAP), mean arterial pressure (MAP) and dirotic notch arterial pressure. Dirotic notch is often used as a characteristic feature of the pressure waveforms in central arteries [42]. All of these estimates, however, rely on the measurement of central aortic pressure, which is uncommon in clinical practice but could be implemented in an ex vivo setup [31]. Moreover, Monge Garcia's research found that the  $E_a$  calculation based on MAP/SV provided a consistent estimation of  $E_a$  with constant bias at multiple peripheral measurement sites [31]. In their calculation, MAP is used as the LV ESP. Hence, would be interesting to see how using these pressures as EPS will affect the output of the developed model.

Also noteworthy is the selection of the  $EDV$ -points for fitting the  $E_a$ -line given that there are reports of using the  $E_a$ -line being fitted from the  $EDV$  at a pressure of 0  $mmHg$  [16]. In the developed model, the line was fitted from the measured pressure at  $EDV$  to the maximal pressure points, but this leads to a different slope of  $E_a$  than fitting a line from  $EDV$  at a pressure of 0 towards the maximal pressure points. Although the slope coming from 0  $mmHg$  would likely be larger and thus further away from the reference value of -2.3,

this is still a notable difference in the calculation of  $E_a$ , which is worth looking into.

A potential way of validating  $E_a$  and  $E_{a_{fit}}$  would be to calculate the elastance per preload for each measurement. This way, one can use a single-beat approach to calculating  $E_a$  which will likely lead to a more accurate value.

The research of Sunagawa et al. described  $E_a$  by use of a formula [38]. They calculated  $E_a$  through the following formula:

$$E_a = \frac{R_c + R}{t_s + \tau[1 - \exp(-t_d/\tau)]} \quad (3)$$

In which  $R_c$  is the characteristic impedance,  $R$  the arterial resistance,  $t_s$  the ejection time,  $\tau$  the time constant of the diastolic arterial pressure decay.  $\tau$  here is equivalent to  $R * C$ , in which  $C$  represents the arterial compliance [38]. Sunagawa et al. then formulated the same equation for end-systolic pressure  $P_{es}$  only by multiplying this formula by  $SV$  which they had defined as  $SV = A_T/(R_c + R)$ . In this equation,  $A_T$  represents the total area under the arterial pressure curve. This led to the following final expression of  $E_a$ :

$$E_a \approx P_{es}/SV = R_T/T \quad (4)$$

In equation 4,  $R_T$  is the total arterial resistance and  $T$  is the cardiac cycle length [38]. Based on this approximation, Sunagawa et al. argued that  $E_a$  can be increased by either increasing the total arterial resistance  $R_T$  or decreasing the cardiac cycle length. The latest would provide a way of validating the  $E_a$  calculations done by the developed model. If one were to increase the  $HR$ , resulting in a decrease in cardiac cycle time  $T$ , the calculated  $E_a$  values of the designed model should increase in magnitude. Furthermore,  $C$  in equation 1 is also dependent on cycle time  $T$ . Since when you shorten the  $T$ , there is less time for the filling of the aorta represented by  $\frac{1}{C} \int (q - q_{Rd}) dt$ . Therefore, one could check whether the  $E_a$  values calculated by the model would decrease at an increase of  $C$ .

Another possibility for validating the  $E_a$  calculations of the developed model would be to increase the total arterial resistance  $R_T$  and check whether the  $E_a$  values of the model increase as well. However, in the current experimental setup, this is not possible yet.

#### 5.2.4 Ratio $E_a/E_{es}$

The ratio  $E_a/E_{es}$  was calculated by the model in order to be able to infer things about the transfer of energy within the heart. Research has found that the mechanical transfer of energy between chambers is optimal at a  $E_a/E_{es}$  ratio of 1 [10]. Other research also states that the  $CWE$  is optimized when the ratio  $E_a/E_{es}$  is around 0.5. Given that the literature search done here found an estimated reference  $E_{es}$  of 1.4 and an  $E_a$  of -2.3, the reference  $E_a/E_{es}$  was set to 1.64. This value favours the measurements with overestimated  $E_a$  and underestimated  $E_{es}$ , but serves mostly to give a perspective of the slopes. Ideally, the ratio would be between 0.5 and 1 for optimal efficiency of energy transfer between the chambers of the heart.

The  $E_{a_{fit}}$  generally performed better with respect to  $E_{es}$  reaching values closer to 1 than the  $E_a/E_{es}$ . The ratio closest to reference value 1.64 was the  $E_{a_{fit}}/E_{es}$  of measurement 2, reaching a calculated ratio of 1.223. The fact that this ratio was the highest can be explained by the fact that the heart of this experiment satisfied the expected properties. Therefore, another measurement of this heart was used as a reference to develop the model, which could explain why the model finds the highest ratio at this measured heart. The second-closest ratio to the reference ratio was found at measurement 5 with an  $E_{a_{fit}}/E_{es}$  of 0.938. This is almost a ratio of 1 indicating that the mechanical efficiency of this heart was quite high.

The  $E_{es}$  of this heart was also the highest of all the measurements, indicating good contractility. The fact that this heart performed the best based on the model is odd, given that the heart had high lactate values at the start of the experiment, which in the clinic would be an indication of an increased chance of mortality due to heart failure [34]. One possible explanation for this heart functioning as well as it did during the measurement could be that it started making use of the high lactate level in the blood as fuel. Lactate has been linked to being an important fuel for myocardial energy production for stressed hearts, which could have temporarily improved the functionality of this heart during the measurement [43]. All in all, the ratio  $E_a/E_{es}$  varied strongly among measurements, which could mean two things. It could either mean that the experimental setup does not mimic bodily afterload as well as it should, leading to increasingly high afterload

affecting the value of both calculated  $E_a$ 's. Or, it could mean that the calculated methods used for  $E_a$  and  $E_{a\text{fit}}$  are inaccurate with respect to  $E_{es}$  or vice versa. Ultimately, this means that this model also requires validation before it can truthfully assess the validity of the experimental model.

### 5.2.5 Calculation of other parameters

Secondary parameters that were calculated were  $EDV$ ,  $ESV$ ,  $EDP$ ,  $ESP$ ,  $SV$ ,  $V_0$  and  $SW$ .  $EDV$  was calculated by taking the maximal volume per cycle.  $EDP$  was the pressure at that point in the cycle.  $ESP$  was calculated by taking the maximal pressure per cycle, with  $ESV$  being the volume at that point in the cycle.  $SV$  was calculated by taking the  $EDV - ESV$ .  $V_0$  was calculated by finding the volume axis intercept at a pressure of 0  $mmHg$ .  $SW$  was calculated by taking the  $SV * (ESP - EDP)$ .

The reference  $EDV$  and  $ESV$  were found in literature based on multiple different experiments and hearts and were therefore rather far apart in terms of the amount of volume. Based on the reference  $EDV$  of 70  $mL$  and  $ESV$  of 11.2  $mL$ , this would mean a reference heart would have an  $SV$  of 58.8  $mL$ . This is a considerable difference between the  $SV$ 's found by the model that were no higher than 13.228  $mL$  and the  $SV$ 's found in literature of around 30-40  $mL$  [14, 22]. This  $SV$  is too large and should therefore not be expected of the sheep hearts used. Hence, it is to be expected that there was some deviation between  $EDV$  and  $ESV$  measured by the model and the reference values.

As already mentioned in section 2.2.2,  $CWE$  is considered an interesting parameter for assessing cardiac functionality. In order for the model to calculate  $CWE$ , the model should also calculate  $PVA$  given that  $CWE = SW/PVA$  [10]. This would also require the model to calculate  $PE$  based on the fact that  $PVA$  can be calculated by adding  $SW$  and  $PE$ . The  $PVA$  is limited by the two lines  $ESPVR$  and  $EDPVR$ . Therefore, the model should also incorporate the  $EDPVR$  in order to calculate the  $PVA$ . The dependency of the  $CWE$  on the other parameters mentioned here is one of the reasons why it was not possible to implement this parameter in the model within the 10-week period of this project. However, given that the ratio  $E_a/E_{es}$  was calculated, the efficiency of the heart can still be assessed, based on the knowledge that  $CWE$  is optimal at an  $E_a/E_{es}$  of 0.5.

Another relevant parameter that could be added to the model is preload-recruitable stroke work ( $PRSW$ ), which reflects the relationship between  $EDV$  and  $SW$  [10].  $PRSW$  is represented as a linear relationship in which the slope reflects the inotropic state. When increasing the administration of inotropic agents such as dobutamine, one would expect the slope of the  $PRSW$  to increase as well [10].  $PRSW$  can be calculated by the formula  $SW/(EDV - V_0)$  [44] Although useful,  $PRSW$  is less sensitive to inotropic state than  $E_{es}$  [10]. Therefore, its added value with respect to the already calculated  $E_{es}$  remains to be proven.

## 5.3 Limitations

First of all, it should be noted that, although the use of the balloon allows for volume measurement of the LV, this measurement is not without flaws. The balloon inflates to roughly the same volume as the LV, but since it cannot be the exact same shape as the inside of the LV, there is still some volume in the LV that is not being measured, thus leading to an inaccuracy in the volume measurements.

A second limitation of the developed model was that the  $E_{es}$  and  $E_a$  were not evaluated as a 3-element Windkessel model as was done by Kelly and Sunagawa et al. [24, 41]. Instead, the model used a simplified calculation based on approximated  $ESP$  points at maximal pressure per cycle and  $EDV$ -points at maximal volume per cycle. As stated, this calculation is simplified and thus does not encapsulate the pressure fluctuations in the LV during filling and ejection. In spite of that, there have been reports of  $ESP/SV$  calculations being consistently equivalent to the more complex Windkessel calculations which plead in favour of the method used in the developed model [45, 46].

A third limitation was concerning the fitting of the balloon in the experimental setup. As can be read from Table 5 in the Appendix, measurements 4 en 5 had problems with fitting the balloon properly on the piston.

This was due to the fact that the plastic cask should be pressed onto the piston at the right angle. Given that this requires a lot of time and some strength, which could afflict the stability of the experimental setup, the balloon was not always perfectly fitted onto the piston. Measurement 4 had a distance of 3.5 *mm* from the top end of the piston to the cask. Considering the diameter of 29 *mm*, this leads to a volume overestimation of the entire measurement of at least 9247.27 *mm*<sup>3</sup>, which is equal to 9.247 *mL*. Similarly, for experiment 5, there was a distance of 3.44 *mm* from the cask to the piston, which leads to a volume overestimation of 9.088 *mL*. Both overestimations were corrected in the model by subtracting the overestimated volume from the measured volume before further analysis of the data. However, the misfitting of the cask might have also led to the balloon not fitting properly in the ventricle, which could have affected the pressure measurements. Given the limited amount of hearts available in the 10-week period of this project, these measurements were included in this project nevertheless. However, one would preferably only use data measured with the balloon properly fitted on the piston. It should be noted that the 5 measurements analysed here were selected out of all the measurements done in the 10-week period based on their merit of having properly formulated PV-loops. This choice of selection was made, because the data was used to build a model assessing heart functionality, which is rather difficult if one uses atypical heart measurements.

A fourth limitation concerned the filling of the piston. During the experiments, the piston was filled with a varying amount of volume per experiment in order to get PV-loops that resembled a healthy heart. The exact amount of volume that was put in the system was not always accurately recorded or fed back to the system, leading to large differences and possible inaccuracies in measured volume among the different experiments. This would explain the large difference in *EDV* that can be seen in Figure 6 and Table 3. Further experiments should take this into account before using the data for analysis so that the hearts in different experiments can be properly compared. It is noteworthy to say though, that this shift in volume does not really matter for the slopes of  $E_{es}$  and  $E_a$ . These can still be an accurate representation of the functionality of the heart.

A fifth limitation of the model concerned the reference values. Although these values were obtained by experiments performed on ovine hearts, most of them were obtained by using a catheter for volume measurement and not a balloon as was the case in this model [26]. Therefore, the reference values of the model should preferably be obtained by using a healthy heart in the same experimental setup with a balloon, given that such a measurement would actually be an adequate reference for assessing the accuracy of the model.

A sixth limitation of the model concerns the actual measurability of the  $E_a$  in this setup. The afterload of the setup is governed by equation 1. The afterload in the setup is set if the values in the equation are also set, which was the case during the experiments. This begs to question if one should truthfully expect a difference in  $E_a$  over the several heart experiments, given that if  $E_a$  truly represents afterload, the measured afterload should always be the same as governed by the parameters in equation 1. If this is indeed the case, measuring the  $E_a$  does not have any added value, since it is a fixed parameter.

Given that this model was developed within a 10-week period, while data was still being collected, the experimental data is only compared to literature-based reference values. However, further implementation of this model should include the comparison of multiple experiments with different prerequisites such as varying dobutamine admission and minimal heart weight for a more constant muscle mass and heart size. Finally, the other parameters mentioned in section 5.2.5 would be a valuable addition to the calculations of the model in order to expand the analysis of cardiac functionality of the model.

## 6 Conclusion

The aim of this project was to develop a predictive model of contractility parameters of the heart based on PV-measurements of sheep hearts in a custom ex-vivo experimental setup. The main aim of the model was to represent the data graphically and calculate the  $ESPVR$ ,  $E_{es}$ ,  $E_a$  and the ratio of  $E_a/E_{es}$ . Given that  $E_a$  is typically calculated for a single heart cycle and the model should represent multiple cycles,  $E_a$  was calculated in two ways leading to parameter  $E_a$  and  $E_{a_{fit}}$ . The calculated parameters were compared to reference values that were obtained through a literature search. Calculated parameter  $E_{es}$ , which was derived of parameter  $ESPVR$ , was considered within an acceptable range of the reference for all measurements but measurement 4. Measurement 4 was suspected of being a heart starting to fail, which would mean that  $E_{es}$  should rightfully not be within the normal range for this measurement, which is what the model reported as output. This can be interpreted as a confirmation of the accuracy of parameter  $E_{es}$  in describing the contractility of the heart. The value of calculated parameter  $E_{a_{fit}}$  was closer to the reference value of  $E_a$  than the calculated  $E_a$  value. However, it should be noted that these reference values were obtained with different experimental setups. Ratio  $E_a/E_{es}$  varied strongly between measurements, which could be interpreted as the experimental setup either not representing afterload well or the calculation of parameters  $E_a$  and  $E_{a_{fit}}$  being inaccurate.

In conclusion, the parameters  $ESPVR$  and  $E_{es}$  calculated by this model were considered accurate in describing the contractility of the hearts based on their PV-measurement. To put contractility in perspective, parameters  $E_a$  and  $E_{a_{fit}}$  were calculated to represent the afterload against which the heart has to pump for ejection to happen. Of these two,  $E_{a_{fit}}$  was considered the more accurate parameter with respect to the reference parameters. However, based on the wide range of the ratio  $E_{a_{fit}}/E_{es}$ , further research still has to show whether  $E_{a_{fit}}$  can actually be considered an adequate calculation of the model that can assess the accuracy of the experimental setup. Accordingly, the developed model still requires validation in order to be sure that it can properly assess cardiac functionality or the accuracy of the experimental setup.

## 7 Appendix

Table 5: Table of experimental remarks for each heart

Measurement	Gender	Age	Start cardioplegia	End cardioplegia	Start SMP	End SMP
1	F	10 months	08:51	08:54	08:59	11:36
2	F	12 months	08:54	09:00	09:05	11:14
3	F	10 months	09:07	09:10	09:16	11:18
4	F	12 months	09:03	09:05	09:10	11:20
5	M	11 months	09:30	09:34	09:40	11:49

Start NMP	Baseline Weight	End SMP Weight	End NMP Weight	Remarks sampling
11:43	286	364	380	Measured after 2 hours of reperfusion
11:24	350	479	502	None
11:32	361	439	x	None
11:32	378	471	503	Problem with balloon fitting
x	402	x	590	Problem with balloon fitting

### 7.1 Script of the developed MATLAB model

```

% Matlab script internship UMCG-XVIVO- Bart Wijntjes- s3453030
% first entry 3-5-2023

%% Clear and Close
clear
close all
clc

%% Data importation

% Import Excel files
[FileName, PathName] = uigetfile('*.xlsx','Select files');
datafile = readtable([PathName FileName]);

% Create arrays for Run time,
Runtime = datafile.('Timestamp');
V = datafile.('Volume_mL_');
P = datafile.('Pressure_mmHg_');
Preload = datafile.('Preload_mmHg_');
InvC = datafile.('x1_C');

t = 1:1:length(Runtime); % t variable

%% smoothing
% Input data: pressure-volume array (pvData)
% Define filter parameters
cutoff_freq = 5; % Adjust the cutoff frequency as desired
sampling_freq = 60; % Adjust the sampling frequency according to your data
nyquist_freq = sampling_freq / 2;

```



```

normalized_cutoff = cutoff_freq / nyquist_freq;

% Apply a low-pass filter to remove noise
[b, a] = butter(4, normalized_cutoff, 'low');
filtered_P = filtfilt(b, a, P);
filtered_V = filtfilt(b, a, V);

% for experiments at which the balloon was not properly fitted onto the
% piston, you can subtract the overestimation in volume here
% filtered_V = filtered_V - 9.088;

% Plot the original and filtered pressure-volume data
figure;
plot(V, P, 'b-', 'LineWidth', 1.5);
hold on;
plot(filtered_V, filtered_P, 'r-', 'LineWidth', 2);
ylabel('Pressure');
xlabel('Volume');
title('Original and Filtered P-V Data');
legend('Original', 'Filtered');

%% find peaks, adjusting the width of the peaks
% find peaks of maxima in pressure in order to determine cyclelength
[pks, locs, w, p] = findpeaks(filtered_P, 'MinPeakProminence', 50, 'Annotate', '
    extents');
% change MinPeakProminence to included/exclude peaks that aren't max
% pressures, generally I used 50
% pks are also the maxima in pressure, locs are the time points

% make a graph to see peaks with their prominence and width to check
figure; findpeaks(filtered_P, t, 'MinPeakProminence', 50, 'Annotate', 'extents')
title('Tryout peak prominence')

% create indices for the cycles based on the locs of the peaks found above
cycle_start_indices = [1; locs];
cycle_end_indices = [locs; length(filtered_V)];
pks_same_length_as_cycles = [1; pks];

% create long V variable for plotting also at negative V
V_neg_plot = -200:1: numel(filtered_V(1:end-201));

% Create smooth P-V cycles
figure;
hold on;
for i = 1:length(cycle_start_indices)-1
    cycle_pressure = filtered_P(cycle_start_indices(i):cycle_end_indices(i)
    );
    cycle_volume = filtered_V(cycle_start_indices(i):cycle_end_indices(i))
    ;

    % Smooth again using a moving average filter
    window_size = 1; % set the window size as desired
    smoothed_pressure = movmean(cycle_pressure, window_size);
    smoothed_volume = movmean(cycle_volume, window_size);

```

```

% store smoothed P and V in a variable
smooth_P(1:length(smoothed_pressure),i) = smoothed_pressure;
smooth_P(smooth_P == 0) = []; % remove zeros
smooth_P = smooth_P(:); % put all in one column

smooth_V(1:length(smoothed_volume),i) = smoothed_volume;
smooth_V(smooth_V == 0) = []; % remove zeros
smooth_V = smooth_V(:); % put all in one column
% smoothing hardly changes the graph w.r.t the filtered data

% create a variable of the filtered V at the locs of the peaks
filt_V_loc_pks = filtered_V(locs);
filt_V_loc_pks_same_length = [1;filtered_V(locs)];

%plot smoothed volume and pressure in a graph
plot(smoothed_volume ,smoothed_pressure , 'LineWidth' , 1.5);

% make polynomial to fit the ESPVR line along maxima of cycles
polynomial = polyfit(filt_V_loc_pks,pks,1); % gives 2 coefficients
% use coefficients to create array that fits along points
slope1 = polynomial(1);
yintercept1 = polynomial(2);

% create variable for ESPVR
slope_func1 = slope1.*filtered_V + yintercept1;

% plot ESPVR in the same graph as smooth P and V
plot(filtered_V,slope_func1,'y','LineWidth',2)
grid minor

E_es = slope1;% store E_es in separate variable for clarity

% calculate EDV
[EDV_cycle,loc_EDV] = max(cycle_volume);
P_at_EDV(i,1) = cycle_pressure(loc_EDV);
EDV_mat(i,1) = EDV_cycle; % store in EDV in matrix
mean_EDV = mean(EDV_mat); % take average EDV

% Store V and P as input for polyfitting Ea later
% Uses pks V-indices and EDV of each cycle
Ea_input_V = [filt_V_loc_pks;EDV_mat];
% uses P of pks and P at EDV of each cycle
Ea_input_P = [pks;P_at_EDV];

% calculate ESV and put it in a matrix
ESV_cycle = min(cycle_volume);
ESV_mat(i,1) = ESV_cycle;
% calculate ESP cycle based on pks (max pressures)
ESP_cycle = pks(i);
% calculate EDP
EDP_cycle = P_at_EDV(i);
% calculate stroke volume

```

```

stroke_volume_cycle = EDV_cycle-ESV_cycle;
stroke_volume_mat(i,1) = stroke_volume_cycle;
% calculate stroke work
% based on the calculations already setup by Utrecht
stroke_work = stroke_volume_cycle*(ESP_cycle-EDP_cycle);
stroke_work_mat(i,1) = stroke_work;
% calculate Ea = ESP/SV based on formula of found in document
% https://hal.science/hal-01123722/document , Page 14
Ea_calculated(i) = ESV_cycle/stroke_volume_cycle;

% calculate Ea per cycle
Ea_cycleP = [ESP_cycle; EDP_cycle];
Ea_cycleV = [filt_V_loc_pks(i);EDV_cycle];
%plot(EDV_cycle,max(cycle_pressure),'or') % plot the maxima with red o
plot(Ea_cycleV,Ea_cycleP,'LineWidth',2,'Color','k');

% make polynomial the fit Ea line along the
Ea_cycle_line = polyfit(Ea_cycleV,Ea_cycleP,1); % gives 2 coefficients
% use coefficients to create array that fits along points
slopeEa_cycle = Ea_cycle_line(1);
mat_slopeEa_cycle(i) = slopeEa_cycle;
mat_intercept_Ea_cycle(i) = Ea_cycle_line(2);
% take mean of slope Ea and intercept of Ea
mean_slopeEa_cycle = mean(mat_slopeEa_cycle);
mean_intercept_Ea_cycle = mean(mat_intercept_Ea_cycle);
% create variable for Ea cycle line
Ea_cycle_func = slopeEa_cycle.*filtered_V + Ea_cycle_line(2);
Ea_mean_cycle_func = mean_slopeEa_cycle*filtered_V +
    mean_intercept_Ea_cycle;

% create longer vector for Ea to plot
Longer_Ea_cycle_func = mean_slopeEa_cycle.*V_neg_plot +...
    mean_intercept_Ea_cycle;

% pick out the middle cycle as a reference cycle for the reference
plot
if i == round(length(cycle_start_indices)/2)

    ref_cycle_P = cycle_pressure;
    ref_cycle_V = cycle_volume;
    ref_peak = pks(i);
    ref_V_loc_peak = filt_V_loc_pks(i);

    ref_EDV = EDV_cycle;
    ref_P_EDV = P_at_EDV(i);

end
end

% make polynomial the fit a line along the Ea_fit
Ea_fit_line = polyfit(Ea_input_V,Ea_input_P,1); % gives 2 coefficients
% use coefficients to create array that fits along points
slopeEa_fit = Ea_fit_line(1);
yinterceptEa_fit = Ea_fit_line(2);

```

```

% create vector for Ea_fit_line to plot
Ea_fit_func = slopeEa_fit.*filtered_V + yinterceptEa_fit;
Longer_Ea_fit_func =slopeEa_fit.*V_neg_plot + yinterceptEa_fit;

%% Fit pressure against volume

% make polynomial the fit a line along maxima of cycles
polynomial = polyfit(filt_V_loc_pks,pks,1); % gives 2 coefficients
% use coefficients to create array that fits along points
slope = polynomial(1);
yintercept = polynomial(2);

% create variable for ESPVR
slope_func = slope.*filtered_V + yintercept;

% create function for Ees_ref
Ees_ref = 1.4 * (V_neg_plot-ref_V_loc_peak) + ref_peak ;

%% find V0, where ESPVR crosses the x-axis
% extrapolate max press peaks for ESPVR
Longer_vector = polyval(polynomial, V_neg_plot);
% Longer_ref_vector = polyval(ref_poly, V_neg_plot);

% indicate sign change is at index loc_V0 of Longer_vector
loc_V0 = find(diff(sign(Longer_vector)));
loc_V0_ref = find(diff(sign(Ees_ref)));

% interpolate values within zero range to get point where ESPVR crosses V
% axis
% find next point after zero crossing
sigPos = logical(Longer_vector>0); % find all positive points
sigPos_ref = logical(Ees_ref>0);
cross = sigPos - circshift(sigPos,1); % find changeover points
ref_cross = sigPos_ref - circshift(sigPos_ref,1);

% assume straight line approximation between adjacent points
crossInd = find(cross); % x indices of cross points
crossInd_ref = find(ref_cross);
nCross = length(crossInd);% number of cross points found
nCross_ref = length(crossInd_ref);
x0 = NaN(1,nCross); % vector of x-values for cross points
x0_ref = NaN(1,nCross_ref);

for aa = 1:nCross
    thisCross = crossInd(aa);
    thisCross_ref = crossInd_ref(aa);

    % interpolate to get x coordinate of approx 0
    x1 = thisCross; % before-crossing x-value
    x2 = thisCross+1; % after-crossing x-value
    y1 = Longer_vector(thisCross); % before-crossing y-value
    y2 = Longer_vector(thisCross+1); % after-crossing y-value

```

```

x1_ref = thisCross_ref; % before-crossing x-value
x2_ref = thisCross_ref+1; % after-crossing x-value
y1_ref = Ees_ref(thisCross_ref); % before-crossing y-value
y2_ref = Ees_ref(thisCross_ref+1); % after-crossing y-value

ratio = (0-y1) / (y2-y1); % interpolate between to find 0
x0(aa) = V_neg_plot(x1) + (ratio*(V_neg_plot(x2)...
    -V_neg_plot(x1))); % estimate of x-value
ratio_ref = (0-y1_ref) / (y2_ref-y1_ref); % interpolate between to
    find 0
x0_ref(aa) = V_neg_plot(x1_ref) + (ratio_ref*(V_neg_plot(x2_ref)...
    -V_neg_plot(x1_ref))); % estimate of x-value

end

% define V0, if V0 cannot be found, expand the range of V_neg_plot
V0 = x0(1);
V0_ref = x0_ref(1);

%% plotting the final graph
figure;
hold on;
grid minor;
plot(filtered_V,filtered_P,'b')
plot(V_neg_plot,Longer_vector,'-g','LineWidth',2)
plot(V_neg_plot,Longer_Ea_cycle_func,'r','LineWidth',2)
%scatter(filt_V_loc_pks,pks,'c') % plotting maxima points
plot(V_neg_plot,Longer_Ea_fit_func,'k','LineWidth',2)

% round of values to 3 decimals for putting in the graphs
rounded_E_es = round(slope1*1000)/1000;
rounded_Ea_cycle = round(mean_slopeEa_cycle*1000)/1000;
rounded_Ea_fit = round(slopeEa_fit*1000)/1000;

% put Ees and V0 in the figure
txt_E_es = sprintf('E_{es} = %5.3f',rounded_E_es); % create text for
    legend
txtplot = text(V0+V0/9,y1*1.5,'E_{es}'); % specify location of 'E_{es}'

txt_V0 = 'V0';
txt_V0_plot = text(V0,-y1,txt_V0); % specify location text 'V0'
plot(V0,0,'or') % mark V0 with red circle

% make text for Ea and Ea_fit
txt_Ea = sprintf('E_a = %5.3f',rounded_Ea_cycle);
txt_Ea_fit = sprintf('E_a {fit} = %5.3f',rounded_Ea_fit);

% limit graph size
xlim([min(filtered_V)-abs(V0*2) max(filtered_V)+5])
ylim([min(filtered_P)-10 max(filtered_P)+10])

% make zero line
yline(0,LineStyle="--");

```

```

% label graphs
legend('Pressure',txt_E_es,txt_Ea,txt_Ea_fit)
xlabel('Volume(mL)');
ylabel('Pressure(mmHg)');

%% plotting the reference graph

Ea_ref_V_input = [ref_V_loc_peak,ref_EDV];
Ea_ref_P_input = [ref_peak,ref_P_EDV];

% make polynomial the fit a line along the Ea_fit
Ea_ref_fixed_slope = polyfit(Ea_ref_V_input,Ea_ref_P_input,1); % gives 2
    coefficients

% use coefficients to create array that fits along points
slopeEa_ref = Ea_ref_fixed_slope(1);
yinterceptEa_ref = Ea_fit_line(2);

% create variable for Ea_fit_line
Ea_ref_func = slopeEa_fit.*filtered_V + ref_peak;

Longer_Ea_ref_func = interp1(Ea_ref_V_input,Ea_ref_P_input,...
    V_neg_plot,'linear','extrap');

% create a variable for Ea with a slope of 2.3
Ea_ref_fixed_slope = -2.3 .* (V_neg_plot-ref_EDV) + 74 ;

% round of values to 3 decimals for putting in the graphs
rounded_ref_E_es = round(1.4*10)/10;
rounded_ref_Ea = round(2.3*10)/10;

% ref text Ees and Ea
ref_txt_Ea = sprintf('E_a = %5.3f',rounded_ref_Ea);
ref_txt_Ees = sprintf('E_{es} = %5.3f',rounded_ref_E_es);

% plotting reference graph
figure;
hold on
grid minor

% put Ees and V0 in the figure
txtplot_ref = text(V0_ref-V0_ref/5,y1_ref*3,'E_{es}');
txt_V0_plot_ref = text(V0_ref,-y1_ref,txt_V0);
plot(V0_ref,0,'or')

plot(ref_cycle_V,ref_cycle_P,'b','LineWidth',2)
plot(V_neg_plot,Ees_ref,'g','LineWidth',2)
%plot(filtered_V,Ea_ref_func,'-k','LineWidth',2)
plot(V_neg_plot,Ea_ref_fixed_slope,'-r','LineWidth',2)
%plot(V_neg_plot,Longer_Ea_ref_func,'y','LineWidth',2)
yline(0,LineStyle="--");
legend('V0','Reference pressure',ref_txt_Ees,ref_txt_Ea)
xlabel('Volume(mL)');

```

```

ylabel('Pressure(mmHg)');

% limit axes of the graph
xlim([min(filtered_V)-abs(V0_ref*2) max(filtered_V)+5])
ylim([min(filtered_P)-10 max(filtered_P)+10])

%% Calculating other parameters
E_es = slope;

% calculating ratio Ea/Ees
RatioEa_fit_Ees = abs(slopeEa_fit/slope1);
RatioEa_cycle_Ees = abs(mean_slopeEa_cycle/slope1);
% calculating EDV_avg,EPV_avg,ESP_avg,EDP_avg
EDV_avg = mean(EDV_mat)
ESV_avg = mean(ESV_mat)
ESP_avg = mean(pks);
EDP_avg = mean(P_at_EDV);
stroke_volume_avg = mean(stroke_volume_mat)
stroke_work_avg = mean(stroke_work_mat)

%% displaying output
fprintf('The Ees has a slope of %0.8f\n', slope1);
fprintf('The mean cycle Ea has a slope of %0.8f\n',mean_slopeEa_cycle);
fprintf('The Ea_fit has a slope of %0.8f\n', slopeEa_fit);
fprintf('Ea/Ees has a ratio of %0.8f\n', RatioEa_cycle_Ees);
fprintf('Ea_fit/Ees has a ratio of %0.8f\n', RatioEa_fit_Ees);

```

## References

- [1] Qianyan Wu et al. “A systematic review and meta-analysis of high-frequency prescription of Zhigancao decoction combined with conventional Western medicine in the treatment of chronic heart failure”. In: (2021). DOI: 10.37766/inplasy2021.6.0098.
- [2] Maryam Vejdani-Jahromi et al. “A Comparison of Acoustic Radiation Force-Derived Indices of Cardiac Function in the Langendorff Perfused Rabbit Heart”. In: *IEEE Transactions on Ultrasonics, Ferroelectrics, and Frequency Control* 63.9 (Sept. 2016), pp. 1288–1295. DOI: 10.1109/tuffc.2016.2543026. URL: <https://doi.org/10.1109/tuffc.2016.2543026>.
- [3] Lynn Raju Punnoose et al. “Implications of Extra-cardiac Disease in Patient Selection for Heart Transplantation: Considerations in Cardiac Amyloidosis”. In: *Cardiac Failure Review* (Jan. 2023). DOI: 10.15420/cfr.2022.24. URL: <https://doi.org/10.15420/cfr.2022.24>.
- [4] Lu Wang et al. “Ex situ heart perfusion: The past, the present, and the future”. In: *The Journal of Heart and Lung Transplantation* 40.1 (Jan. 2021), pp. 69–86. DOI: 10.1016/j.healun.2020.10.004. URL: <https://doi.org/10.1016/j.healun.2020.10.004>.
- [5] John Louca et al. “The international experience of in-situ recovery of the DCD heart: a multicentre retrospective observational study”. In: *eClinicalMedicine* 58 (Apr. 2023), p. 101887. DOI: 10.1016/j.eclinm.2023.101887. URL: <https://doi.org/10.1016/j.eclinm.2023.101887>.
- [6] A. Ciarka et al. “DCD Donor Hearts Recipients Compared to DBD Donor Heart Recipients Present with Comparable Systolic Left Ventricular Function and Better Myocardial Strain at 1 Year Follow Up”. In: *The Journal of Heart and Lung Transplantation* 38.4 (Apr. 2019), S26–S27. DOI: 10.1016/j.healun.2019.01.049. URL: <https://doi.org/10.1016/j.healun.2019.01.049>.
- [7] Robert M. Bell, Mihaela M. Mocanu, and Derek M. Yellon. “Retrograde heart perfusion: The Langendorff technique of isolated heart perfusion”. In: *Journal of Molecular and Cellular Cardiology* 50.6 (June 2011), pp. 940–950. DOI: 10.1016/j.yjmcc.2011.02.018. URL: <https://doi.org/10.1016/j.yjmcc.2011.02.018>.
- [8] Michael I. Brener et al. “Invasive Right Ventricular Pressure-Volume Analysis: Basic Principles, Clinical Applications, and Practical Recommendations”. In: *Circulation: Heart Failure* 15.1 (Jan. 2022). DOI: 10.1161/cirheartfailure.121.009101. URL: <https://doi.org/10.1161/cirheartfailure.121.009101>.
- [9] David P. Stonko et al. “TEVAR Acutely Augments LV Biomechanics in An Animal Model: A mechanism for post-operative heart failure and hypertension”. In: *Annals of Vascular Surgery* (Apr. 2023). DOI: 10.1016/j.avsg.2023.04.007. URL: <https://doi.org/10.1016/j.avsg.2023.04.007>.
- [10] Dima Rodriguez. “Left Ventricular Pressure-Volume Analysis: an example of function assessment on a sheep”. PhD thesis. Université Paris Sud, 2015.
- [11] Tamas Seres. “Heart Failure”. In: *Anesthesia Secrets*. Elsevier, 2011, pp. 236–243. DOI: 10.1016/b978-0-323-06524-5.00035-0. URL: <https://doi.org/10.1016/b978-0-323-06524-5.00035-0>.
- [12] J L Weiss, J W Frederiksen, and M L Weisfeldt. “Hemodynamic determinants of the time-course of fall in canine left ventricular pressure.” In: *Journal of Clinical Investigation* 58.3 (Sept. 1976), pp. 751–760. DOI: 10.1172/jci108522. URL: <https://doi.org/10.1172/jci108522>.
- [13] S K Varma et al. “Is tau a preload-independent measure of isovolumetric relaxation?” In: *Circulation* 80.6 (Dec. 1989), pp. 1757–1765. DOI: 10.1161/01.cir.80.6.1757. URL: <https://doi.org/10.1161/01.cir.80.6.1757>.
- [14] Roy R. Ha et al. “An Integrative Cardiovascular Model of the Standing and Reclining Sheep”. In: *Cardiovascular Engineering* 5.2 (June 2005), pp. 53–76. DOI: 10.1007/s10558-005-5341-0. URL: <https://doi.org/10.1007/s10558-005-5341-0>.
- [15] Fabrice Bauer et al. “Left ventricular outflow tract mean systolic acceleration as a surrogate for the slope of the left ventricular end-systolic pressure-volume relationship”. In: *Journal of the American College of Cardiology* 40.7 (Oct. 2002), pp. 1320–1327. DOI: 10.1016/s0735-1097(02)02138-1. URL: [https://doi.org/10.1016/s0735-1097\(02\)02138-1](https://doi.org/10.1016/s0735-1097(02)02138-1).



- [16] T Kameyama et al. “Energy conversion efficiency in human left ventricle.” In: *Circulation* 85.3 (Mar. 1992), pp. 988–996. DOI: 10.1161/01.cir.85.3.988. URL: <https://doi.org/10.1161/01.cir.85.3.988>.
- [17] Mark R. Starling. “Left ventricular-arterial coupling relations in the normal human heart”. In: *American Heart Journal* 125.6 (June 1993), pp. 1659–1666. DOI: 10.1016/0002-8703(93)90756-y. URL: [https://doi.org/10.1016/0002-8703\(93\)90756-y](https://doi.org/10.1016/0002-8703(93)90756-y).
- [18] Ch. Jacoby et al. “Direct comparison of magnetic resonance imaging and conductance microcatheter in the evaluation of left ventricular function in mice”. In: *Basic Research in Cardiology* 101.1 (Aug. 2005), pp. 87–95. DOI: 10.1007/s00395-005-0542-7. URL: <https://doi.org/10.1007/s00395-005-0542-7>.
- [19] Sanaz Hatami et al. “Myocardial Functional Decline During Prolonged Ex Situ Heart Perfusion”. In: *The Annals of Thoracic Surgery* 108.2 (Aug. 2019), pp. 499–507. DOI: 10.1016/j.athoracsur.2019.01.076. URL: <https://doi.org/10.1016/j.athoracsur.2019.01.076>.
- [20] Patrick Segers et al. “Predicting systolic and diastolic aortic blood pressure and stroke volume in the intact sheep”. In: *Journal of Biomechanics* 34.1 (Jan. 2001), pp. 41–50. DOI: 10.1016/s0021-9290(00)00165-2. URL: [https://doi.org/10.1016/s0021-9290\(00\)00165-2](https://doi.org/10.1016/s0021-9290(00)00165-2).
- [21] G L Freeman and J T Colston. “Role of ventriculovascular coupling in cardiac response to increased contractility in closed-chest dogs.” In: *Journal of Clinical Investigation* 86.4 (1990), pp. 1278–1284. DOI: 10.1172/jci114835.
- [22] Róbert Romvári et al. “Heart performance of lambs and its relation to muscle volume and body surface”. In: *Turkish Journal of Veterinary and Animal Sciences* 39 (2015), pp. 69–74. DOI: 10.3906/vet-1403-92. URL: <https://doi.org/10.3906/vet-1403-92>.
- [23] Daniel J. Penny, Jonathan P. Mynard, and Joseph J. Smolich. “Aortic wave intensity analysis of ventricular-vascular interaction during incremental dobutamine infusion in adult sheep”. In: *American Journal of Physiology-Heart and Circulatory Physiology* 294.1 (Jan. 2008), H481–H489. DOI: 10.1152/ajpheart.00962.2006. URL: <https://doi.org/10.1152/ajpheart.00962.2006>.
- [24] R P Kelly et al. “Effective arterial elastance as index of arterial vascular load in humans.” In: *Circulation* 86.2 (Aug. 1992), pp. 513–521. DOI: 10.1161/01.cir.86.2.513. URL: <https://doi.org/10.1161/01.cir.86.2.513>.
- [25] Tomoki Kameyama et al. “Ventricular load optimization by unloading therapy in patients with heart failure”. In: *Journal of the American College of Cardiology* 17.1 (Jan. 1991), pp. 199–207. DOI: 10.1016/0735-1097(91)90728-r. URL: [https://doi.org/10.1016/0735-1097\(91\)90728-r](https://doi.org/10.1016/0735-1097(91)90728-r).
- [26] Takahiro Nishida et al. “The Effect of Sudden Failure of a Rotary Blood Pump on Left Ventricular Performance in Normal and Failing Hearts”. In: *Artificial Organs* 24.11 (Nov. 2000), pp. 893–898. DOI: 10.1046/j.1525-1594.2000.06549.x. URL: <https://doi.org/10.1046/j.1525-1594.2000.06549.x>.
- [27] Ethan O. Kung and Charles A. Taylor. “Development of a Physical Windkessel Module to Re-Create In Vivo Vascular Flow Impedance for In Vitro Experiments”. In: *Cardiovascular Engineering and Technology* 2.1 (Nov. 2010), pp. 2–14. DOI: 10.1007/s13239-010-0030-6. URL: <https://doi.org/10.1007/s13239-010-0030-6>.
- [28] The MathWorks Inc. *MATLAB version: 9.13.0 (R2022b)*. Natick, Massachusetts, United States, 2022. URL: <https://www.mathworks.com>.
- [29] Hiroyuki Suga, Kiichi Sagawa, and Artin A. Shoukas. “Load Independence of the Instantaneous Pressure-Volume Ratio of the Canine Left Ventricle and Effects of Epinephrine and Heart Rate on the Ratio”. In: *Circulation Research* 32.3 (Mar. 1973), pp. 314–322. DOI: 10.1161/01.res.32.3.314. URL: <https://doi.org/10.1161/01.res.32.3.314>.
- [30] URL: <https://nl.mathworks.com/help/matlab/>.

- [31] Manuel Ignacio Monge Garcia et al. “Reliability of effective arterial elastance using peripheral arterial pressure as surrogate for left ventricular end-systolic pressure”. In: *Journal of Clinical Monitoring and Computing* 33.5 (Dec. 2018), pp. 803–813. DOI: 10.1007/s10877-018-0236-y. URL: <https://doi.org/10.1007/s10877-018-0236-y>.
- [32] K Hayashi et al. “Single-beat estimation of ventricular end-systolic elastance-effective arterial elastance as an index of ventricular mechanoenergetic performance”. en. In: *Anesthesiology* 92.6 (June 2000), pp. 1769–1776.
- [33] Alexa S. Hendricks et al. “Central ANG-(1–7) infusion improves blood pressure regulation in antenatal betamethasone-exposed sheep and reveals sex-dependent effects on oxidative stress”. In: *American Journal of Physiology-Heart and Circulatory Physiology* 316.6 (June 2019), H1458–H1467. DOI: 10.1152/ajpheart.00497.2018. URL: <https://doi.org/10.1152/ajpheart.00497.2018>.
- [34] Chiara Lazzeri et al. “Clinical significance of Lactate in acute cardiac patients”. In: *World Journal of Cardiology* 7.8 (2015), p. 483. DOI: 10.4330/wjc.v7.i8.483. URL: <https://doi.org/10.4330/wjc.v7.i8.483>.
- [35] M Takeuchi et al. “Single-beat estimation of the slope of the end-systolic pressure-volume relation in the human left ventricle.” In: *Circulation* 83.1 (Jan. 1991), pp. 202–212. DOI: 10.1161/01.cir.83.1.202. URL: <https://doi.org/10.1161/01.cir.83.1.202>.
- [36] Naomi Wo et al. “Assessment of single beat end-systolic elastance methods for quantifying ventricular contractility”. In: *Heart and Vessels* 34.4 (Nov. 2018), pp. 716–723. DOI: 10.1007/s00380-018-1303-5. URL: <https://doi.org/10.1007/s00380-018-1303-5>.
- [37] Knut E. Kjørstad, Christian Korvald, and Truls Myrmel. “Pressure-volume-based single-beat estimations cannot predict left ventricular contractility in vivo”. In: *American Journal of Physiology-Heart and Circulatory Physiology* 282.5 (May 2002), H1739–H1750. DOI: 10.1152/ajpheart.00638.2001. URL: <https://doi.org/10.1152/ajpheart.00638.2001>.
- [38] K Sunagawa, W L Maughan, and K Sagawa. “Optimal arterial resistance for the maximal stroke work studied in isolated canine left ventricle.” In: *Circulation Research* 56.4 (Apr. 1985), pp. 586–595. DOI: 10.1161/01.res.56.4.586. URL: <https://doi.org/10.1161/01.res.56.4.586>.
- [39] Manuel Ignacio Monge Garcia, Paula Saludes Orduña, and Maurizio Cecconi. “Understanding arterial load”. In: *Intensive Care Medicine* 42.10 (Jan. 2016), pp. 1625–1627. DOI: 10.1007/s00134-016-4212-z. URL: <https://doi.org/10.1007/s00134-016-4212-z>.
- [40] Wilmer W. Nichols and Michael F. O’Rourke. *McDonald’s blood flow in arteries: Theoretical, experimental and clinical principles*. Hodder Arnold, 2005.
- [41] K. Sunagawa et al. “Left ventricular interaction with arterial load studied in isolated canine ventricle”. In: *American Journal of Physiology-Heart and Circulatory Physiology* 245.5 (Nov. 1983), H773–H780. DOI: 10.1152/ajpheart.1983.245.5.h773. URL: <https://doi.org/10.1152/ajpheart.1983.245.5.h773>.
- [42] Mazen Abou Gamrah et al. “Mechanics of the aortic notch: An acceleration hypothesis”. In: *Proceedings of the Institution of Mechanical Engineers, Part H: Journal of Engineering in Medicine* 234.11 (May 2020), pp. 1253–1259. DOI: 10.1177/0954411920921628. URL: <https://doi.org/10.1177/0954411920921628>.
- [43] J Hutter et al. “Inhibition of fatty acid oxidation and decrease of oxygen consumption of working rat heart by 4-bromocrotonic acid”. In: *Journal of Molecular and Cellular Cardiology* 16.1 (Jan. 1984), pp. 105–108. DOI: 10.1016/s0022-2828(84)80718-x. URL: [https://doi.org/10.1016/s0022-2828\(84\)80718-x](https://doi.org/10.1016/s0022-2828(84)80718-x).
- [44] Wen-Shin Lee et al. “Estimation of preload recruitable stroke work relationship by a single-beat technique in humans”. In: *American Journal of Physiology-Heart and Circulatory Physiology* 284.2 (Feb. 2003), H744–H750. DOI: 10.1152/ajpheart.00455.2002. URL: <https://doi.org/10.1152/ajpheart.00455.2002>.

- [45] Denis Chemla et al. “Contribution of systemic vascular resistance and total arterial compliance to effective arterial elastance in humans”. In: *American Journal of Physiology-Heart and Circulatory Physiology* 285.2 (Aug. 2003), H614–H620. DOI: 10.1152/ajpheart.00823.2002. URL: <https://doi.org/10.1152/ajpheart.00823.2002>.
- [46] Patrick Segers, Nikos Stergiopoulos, and Nico Westerhof. “Relation of effective arterial elastance to arterial system properties”. In: *American Journal of Physiology-Heart and Circulatory Physiology* 282.3 (Mar. 2002), H1041–H1046. DOI: 10.1152/ajpheart.00764.2001. URL: <https://doi.org/10.1152/ajpheart.00764.2001>.